Invariance and variability in interaction error-related potentials and their consequences for classification

Mohammad Abu-Alqumsan[1], Christoph Kapeller[2,3], Christoph Hintermüller[2,3], Christoph Guger[2,3] and Angelika Peer[4]

[1] Chair of Automatic Control Engineering, Technical University of Munich (TUM), Munich, Germany
[2] Guger Technologies OG, Graz, Austria
[3] g.tec medical engineering GmbH, Schiedlberg, Austria
[4] Bristol Robotics Laboratory, University of the West of England, Bristol, UK

E-mail: moh.marwan@lsr.ei.tum.de

Abstract.
Objective. This paper discusses the invariance and variability in interaction error-related potentials (ErrPs), where a special focus is laid upon the factors of (1) the human mental processing required to assess interface actions (2) time (3) subjects. *Approach.* Three different experiments were designed as to vary primarily with respect to the mental processes that are necessary to assess whether an interface error has occurred or not. The three experiments were carried out with 11 subjects in a repeated-measures experimental design. To study the effect of time, a subset of the recruited subjects additionally performed the same experiments on different days. *Main results.* The ErrP variability across the different experiments for the same subjects was found largely attributable to the different mental processing required to assess interface actions. Nonetheless, we found that interaction ErrPs are empirically invariant over time (for the same subject and same interface) and to a lesser extent across subjects (for the same interface). *Significance.* The obtained results may be used to explain across-study variability of ErrPs, as well as to define guidelines for approaches to the ErrP classifier transferability problem.

Keywords: EEG, BCI, Error-related Potentials, P300, invariance, classification

Submitted to: *J. Neural Eng.*

1. Introduction

Error processing and awareness mechanisms in the brain lead to reproducible brain activity patterns, which can be observed in scalp EEG time-locked to events of errors. In general, these patterns are referred to as error-related potentials (ErrPs) and are typically taxonomized into four types: *response*, *observation*, *feedback* and *interaction* ErrPs [1, 2]. This taxonomy basically reflects the variability in the error potentials with respect to changes in the tasks, in which they have been observed. *Response* ErrPs were found to be elicited after incorrect responses in speeded choice reaction time (RT) tasks [3,4]. *Observation* ErrPs, on the other hand, have been shown to be elicited after observing errors committed by other humans [5] or virtual devices [6,7] in different tasks including speeded choice RT. *Feedback* ErrPs are elicited after negative feedback (e.g. feedback of unfavorable results in time estimation tasks) [8–10]. Finally, *interaction* ErrPs were reported after feedback that indicates erroneous interface actions [11, 12], and therefore they can be thought of as a special case of *observation* and *feedback* ErrPs.

The average difference waveform in the event-related potential (ERP) structure between the error and correct trials (error-minus-correct) is usually used to highlight the ErrP components. For instance, the difference waveform of response ErrPs has been characterized by Falkenstein et al. [3] with a negativity Ne (sometimes referred to as error-related negativity ERN) and a later, more extended positivity Pe. The sharp negative component, Ne, peaked at about 80 ms and was maximal at midline frontocentral scalp locations, whereas the positivity, Pe, peaked in the interval 200-500 ms after incorrect key presses [13]. The Pe was shown in a more recent study to have two subcomponents, with frontocentral and centroparietal distributions [14]. The negativity was also observed in correct trials, however with smaller amplitudes (referred to as correct-related negativity CRN). According to [13], the presence of CRN might indicate that the negativity Ne reflects the comparison process itself (between the correct and performed response) and not its outcome, and that the independent component Pe reflects a later aspect of the error processing, e.g. error awareness [14, 15].

In addition to the temporal (phase-locked) signature of errors in scalp EEG, spectral (phase- and non-phase-locked) signatures were observed starting just before incorrect presses in speeded motor responses manifested as an increase in mid-frontal theta band activity accounting for 57% of ERN peak amplitude [16], and an increase in delta-power [4]. The respective temporal and/or spectral signatures may vary across the different types of ErrPs; nonetheless, independent of the specific type of error potentials and independent of the task performed, EEG and fMRI studies in humans [8, 13, 17–19] and single-unit studies in monkeys [20, 21] have suggested the anterior cingulate cortex (ACC), the supplementary motor Area (SMA), and/or pre-SMA (all in the posterior medial frontal cortex, pMFC) as candidates for a common neural generator. This in turn suggests that the different ErrP types are manifestations of similar performance monitoring systems [22–25]. Furthermore, errors, and more specifically, conscious errors, are accompanied by changes in autonomic activity, like heart rate deceleration, increase in pupil size, larger skin conductance responses and increased amygdala activity [15].

Schalk et al. [11] were the first to report that EEG signals that follow erroneous and correct selections by a computer interface differ significantly. The term *interaction* ErrPs has been coined later by Ferrez et al. [12] to refer to this type of ErrPs. Thereafter, there has been a special interest in *interaction* ErrPs within the field of brain-computer interfaces (BCIs), that concerns itself with providing users, particularly those living with disabilities, with control and communication abilities on the basis of their measurable brain neural activity. Hereby, the presence or absence of *interaction* ErrPs in scalp EEG can be used as a means to respectively invalidate or validate a first-stage BCI selection. The first selection can be mediated based on P300, SSVEP or motor-imagery (MI) signals, whose classification is known to be prone to errors due to the inherent presence of noise in scalp EEG. The amplitude of the noise (background activity in the brain and bodily artifacts) can be of several orders of magnitude above the amplitude of ERPs [26, 27].

First efforts to decrease error rates during BCI-mediated interaction considered adding a response verification (RV) step [28], where users needed to confirm each selection by communicating an additional one to the system. Reducing the time required for the verification step might lead to improvements in the bit rate in addition to the accuracy improvement. It can be shown, nonetheless, that if the interface parameters remain the same (i.e. with respect to the number of interface elements, time for a single selection, interaction paradigm, etc.) for both the selection and verification steps, a significant loss in achievable bit rates is then expected for almost all levels of single trial accuracies (see the supplementary material for more details). On the other hand, integrating the detection of ErrPs into different practical BCI systems [11, 12, 29–33] improved both the accuracy and the achieved bit rates. High false alarm (i.e. estimating trials as erroneous when they are not) rates, however, may degrade the achieved bit rate and interaction speed [32].

Typically, training sessions that contain a considerable amount of ErrP/noErrP examples are used to learn classification boundaries that separate the two classes. For the different types of BCIs, including those based on ErrPs, it is generally desirable to reuse previously recorded sessions in training classifiers that can be used across different tasks, on different days, or/and with different subjects [34]. This is, however, made difficult, with the considerable (between and within-subjects) fluctuations in the underlying statistics of the brain patterns under consideration [35, 36]. Fluctuations, due to the non-stationarity dynamics of the brain, may result in trial-to-trial variability [37] and latency jitter of the ERP components on session-to-session basis [38] and may lead to reduced accuracy levels when going from the calibration (i.e. training) phase of classifiers to their online usage, even with the same subjects, on the same days and with the same interfaces/tasks [36, 39].

However, and apart from the EEG non-stationarity, there exist *invariant* features that make ErrPs visible and reproducible in the first place. In the present work, it is investigated whether there are invariants of *interaction* ErrPs and the consequences these invariants, if any, might have for their classification. Our main focus was to check possible invariants with respect to: (1) human mental processes that are required after feedback onset (2) time (3) subjects.

The *variability* in *interaction* ErrPs across the different levels of a certain experimental factor is expressed hereby in terms of the observed differences in the temporal evolution and morphology of the average ErrP waveforms. The notion of *invariance*, on the other hand, is used throughout this work as underlying this very notion of variability. Hereby, the association between the two terms is similar to that in studies of speech processes (e.g. [40]), where despite the existing between and within-talker variability with respect to speech signals (e.g. vocal pitch, volume, fluency), there are invariant features that allow their listeners to recognize the intended meaning. By analogy, it is reasoned here that should there exist some statistically invariant features of *interaction* ErrPs across the different levels of a certain experimental factor, then data obtained at a certain level can be used reliably to draw a linear plane separating error and correct trials obtained at different level(s). Invariance with respect to a specific factor is hereby measured with the accuracy of classifier transfer across the different levels of this factor. Classification accuracies are quantified by the *normalized mutual information* (NMI), which is used to summarize the classification sensitivity and specificity with a single metric [2].

In order to answer the questions raised above, three different experiments and tasks were designed and conducted with different subjects. The first experiment is quite similar to the keyboard-based cursor movement in [12] and the other two experiments, similar to [30], were based on P300-mediated interaction. Some closely related work to ours exists in [41] for *observation* ErrPs and [42] for different types of errors. The main result of this work is that we show that *interaction* ErrPs (1) are highly sensitive with respect to the mental processing required to assess interface actions (2) are quite empirically invariant over time for the same interface (3) have invariant features across subjects for the same interface. It is also observed that ErrPs are sensitive to the details of the EEG preprocessing pipeline. This may explain the ErrP variability across studies of similar nature regarding the mental processes of the interface actions.

Prior research on ErrPs have partially tackled some of these issues at separate occasions (see Section 2), which helped to formulate first hypotheses and guided the design of the three interfaces/experiments. With this work, the aim is to ground irrelevant factors in the experimental design and in the pre-processing pipeline so that concrete conclusions can be drawn with respect to the different sources of invariance and variability under consideration. To the best of our knowledge, this is the first work that tackles such sources from a unified perspective.

This paper is structured as follows. Section 2 provides a short review on related work and similar experiments to ours. Section 3 reports the materials and the design of the different experiments conducted in this work. Experimental results are presented in section 4 followed by a discussion in section 5. This paper concludes with section 6.

2. Related work

There is a plethora of work in the literature that examined the presence of *interaction* ErrPs and their detection with many different interfaces and tasks.

Across these studies, one can observe that many aspects remained invariant whereas many others have shown great variability. The current work builds on findings from these studies and tries to extend our understanding of the sources of variability and invariance in *interaction* ErrPs.

2.1. Invariance with respect to human mental processes consequent to the feedback onset

In one-dimensional cursor control using MI-based BCI (based on modulation of μ and β rhythms) [11], it has been shown that the difference waveform (error-minus-correct) is characterized by a positive potential centered at the vertex peaking around 180 ms. Despite that the cursor was required to be moved incrementally towards the goal, the error and correct trials were defined solely based on the correctness of the final destination. In quite similar experiments [12], the MI-based interface was simulated by keyboard presses and each intermediate step towards the goal was labeled either as a correct or erroneous trial. The difference waveform time-locked to cursor movements (i.e. feedback onset) was shown to have a sharp negative peak after 250 ms (N2) followed by a positive peak after 320 ms (P3) and a second broader negative peak after 450 ms (N4). These peaks clearly differ from the positive potential in [11], and this discrepancy can be attributed to the different mental processes required to evaluate whether or not a cursor arrives at the target goal and whether or not it just moves towards it [29].

Similarly, in experiments where subjects observed and evaluated the movements of a virtual device towards cued goals, Iturrate et al. [41] have shown that slight changes in the performed tasks lead to significant differences in the peak latency of N2, P3 and P4 in *observation* ErrPs. The tasks differed only in the way the virtual device moved with respect to the cued goals (either with incremental steps in a horizontal and vertical grids or with a single jump). The observed signal variations were shown additionally, to make it difficult for a classifier trained with data from one task to straightforwardly transfer to other ones. Yet, recalibration and adaptation of the learned classifier (by adapting the means of correct and incorrect trials to the new task) provided fairly good results when a few training examples for the new task were available [41]. Further, using three different experimental protocols in [43], where users evaluated the movements of a virtual square, a simulated robotic arm and a real robot arm, differences in peak latencies of P3 and N4 in *observation* ErrPs across these experiments were reported to be significant, whereas differences in peak amplitudes were not. As the average waveforms of correct and error trials were observed to be similar with respect to the general shape across experiments, correcting single trial data for the observed latency differences was shown to enhance classifier generalizability across tasks.

Furthermore, in a simple video game task with continuous feedback, where users used a gamepad to control a cursor to avoid collisions with blocks dropping from the top of the screen with constant speeds, different kinds of errors were found to produce different and distinguishable ErrP waveforms with different spectral contents [2, 42]. The examined errors were either due to inaccurate feedback (i.e. cursor moved deliberately in directions that differ from the user input) or due to failing to achieve target goals (i.e. user input led to collisions with the moving objects). The two errors were respectively referred to by the authors as *execution* and *outcome* errors. Our thinking is that such differences in the morphology of the difference waveforms across the two types of errors stem from the different mental processes required to assess the feedback stimuli. In particular, the shape and the scalp topography of *execution errors* are reported to have N2, P3 and N4 components, similar to those reported in *interaction* ErrPs [12] and *observation* ErrPs [41], where judging the correctness of interface actions is achieved by mentally evaluating whether a cursor moved as signaled/expected or not.

On a different vein, some variability in the ErrP waveforms can be observed across hybrid P300-ErrP systems, where different feedback presentation methods have been deployed. For instance, authors in [29, 44, 45] adopted a central feedback presentation, whereby the selected character was shown overlaid at the center of the spelling matrix, 1 second or more after the row-column flashing is stopped. The central feedback strategy was also employed in a modified way in [30], where the character presentation is preceded by a presentation of an empty square at the center of the display aiming at attracting the user visual attention to that spot before the estimated character is presented at the same location on the display. This way, ocular artifacts can be reduced. The observed grand average difference waveform at Cz for a group of healthy subjects was characterized by a negativity at around 348 ms and a later positivity at around 465 ms [30]. Alternatively, the feedback in [46] was done by replacing all the matrix elements with the estimated one.

It can be observed from this short review of the available hybrid P300-ErrP systems that the main concern of designing the feedback presentation was to avoid possible ocular artifacts that may accompany the onset of the feedback. However, we argue that changing the style of feedback presentation leads also to recruiting different mental processes to assess the feedback stimulus, and therefore observed ErrPs signals vary as a byproduct. For instance, the central feedback, when used in language spelling tasks, requires that the users remember (though for a very short time) the last character, to which they attended, and compare it with the estimated one. Users may not need to perform this comparison (or even memorization) when the replacement feedback in [46] is used, since in this case a visual change of the character at the attended place in the P300 matrix simply means that the interface made an error. Consequently, one can observe a great discrepancy in the two ErrP waveforms in [30] and [46] (polarities of the different peaks in the two signals appear to be reversed).

2.2. Invariance with respect to user input

In an attempt to reduce the time required to collect ErrP/noErrP training data, Schmidt et al. [32] have designed a calibration keyboard-based experiment for the P300 center speller [47], in which the post-feedback behavior of the interface is identical to that in the P300 case. This way, authors make sure that the mental processes required to assess the feedback as correct/erroneous are identical across the keyboard-calibration and P300-online conditions. Herein, visual inspection of the grand averages of the erroneous and correct trials reveals a great similarity across the two tasks with respect to the general shape. However, the error negativity (Ne) and positivity (Pe) of the difference waveform were observed with stronger amplitudes and earlier in time in the online condition compared to calibration. A linear discriminant analysis (LDA) classifier for *interaction* ErrPs trained with data from the calibration experiments was shown to transfer, however with a reduced performance, to the P300-based online sessions.

Furthermore, Kim and Kirchner [7] designed a task to compare *observation* ErrPs (users observed the movement of a cursor with no input whatsoever) and *interaction* ErrPs (users controlled the movement of a cursor with a noisy keyboard). Hereby, *interaction* ErrPs appeared after cursor movements in directions that do not match the user's keyboard presses, while *observation* ErrPs appeared when an observed agent moved in directions that deviate from a hard-coded path. It was observed that the grand average difference waveforms of the two ErrP types have similar shapes in the early time region 0.16-0.4 s, but exhibit different shapes in the late time region 0.4-0.8 s. Arguably, this discrepancy might be attributed to the overlap of errenous and correct trials as a result of the used experimental paradigms, and/or the fact that the two tasks differed in that key presses were self-paced in the interaction task and hard-coded within predefined intervals in case of the observed agent. The authors have shown that a linear support vector machine (SVM) classifier learned from the *observation* ErrPs can successfully transfer to *interaction* ErrPs. The classifier transfer in the reverse direction (i.e. from interaction to observation) was also successful but with a reduced performance.

Taking advantage of these results, it may be assumed that if two tasks differed with respect to the type of the user input, and a sufficient time gap was introduced between the arrival time of the user input and the onset time of the feedback stimulus, then any observed variability in the ErrP waveforms consequent to the feedback onset across the two tasks is most likely caused by other factors than the discrepancy in user input.

2.3. Invariance with respect to time

Ferrez et al. [12] have shown *interaction* ErrPs to be stable over time as the average difference waveforms and scalp topographies remained similar for two recordings spaced about three months apart. Additionally, a Gaussian classifier trained with data from the first recording was reported to produce relatively high accuracy levels (about 80%) when applied on the data from the second recording.

2.4. Invariance with respect to subjects

It is argued in [48] that ERN is a subjective response that is influenced by individual differences in cognitive modeling of what is being correct/incorrect. This is supported by evidences from different studies which show e.g. that the magnitude of ERN is correlated with the level of academic performance of subjects [24] and that the level of ACC and pre-SMA activation and magnitude of ERN is correlated with age [49, 50].

However, despite this inter-subject variability, no significant difference in peak latency or peak-to-peak amplitude of *interaction* ErrPs has been observed across the groups of healthy and motor-impaired subjects [30]. Further, it has been shown in [7, 51] that a classifier learned from examples of *interaction* ErrPs obtained from the EEG of several subjects time-locked to erroneous/correct interactions can transfer to new subjects performing the same task with relatively good accuracy (75% on average). The across-subjects classifier transfer, for most subjects, performed worse than a classifier transfer among different types (observation to interaction and vice versa) of ErrPs within the same subjects [7].

3. Material and methods

It can be summarized from the previous review that the *interaction* ErrPs exhibit some invariance across subjects and over time, which was also confirmed with the possible classifier transfer across these factors. In this work, we argue that the discrepancy in the mental processes required to assess interface actions accounts for much of the variability observed across different studies. This hypothesis is tested in the present work using a repeated-measures experimental design, where the same subjects performed three experiments on different days. The tasks in two experiments are designed to be exactly the same, except for the way the visual feedback is provided to users. Additionally, to ground the effect of time, a small sample of the recruited participants performed the same experiments, for multiple times on different days.

3.1. Subjects

A total of 11 healthy adults (7 male, 4 female) aged 27.4 ± 5.7 (range $19 - 39$) served as paid volunteer subjects in this study. S10 was left-handed and all subjects except S2 had normal or corrected-to-normal vision. Subject S2 had extreme hyperopia in the left eye. All subjects were naïve as to the purposes of the experiments. Subject S11 was excluded from the study for not being able to use the P300 speller.

3.2. Data recording

During the different experiments, the participants were seated 0.7 m away from an LCD monitor on a comfortable armchair in a slightly dimmed room. All participants gave their written informed consent. Participants were additionally asked to fill in pre- and post-questionnaires, that were meant to collect data about the level of tiredness before and after the experiment in addition to some demographical data. This data, however, was not used for the purposes of this study.

Scalp EEG signals were recorded from 28 electrodes positioned according to the international extended 10/20 electrode system at F7, F3, Fz, F4, F8, FC5, FC1, FCz, FC2, FC6, T7, C3, Cz, C4, T8, CP5, CP1, CPz, CP2, CP6, P7, P3, Pz, P4, P8, PO7, POz and PO8 as shown in figure 1. Similar to [52, 53], Electrooculogram (EOG) traces were obtained from electrodes F9, F10, FP2 and an additional electrode placed directly below the right eye. EEG and EOG electrodes were referenced to the right earlobe and the ground electrode was positioned at FPz. The horizontal bipolar EOG (HEOG) signal was computed from the raw data of electrodes F9 and F10. Similarily, vertical bipolar EOG (VEOG) was computed from FP2 and the electrode placed below the right eye.

EEG and EOG data were measured with sampling rate of 256 Hz at full DC using g.USBamp acquisition system (g.tec medical engineering GmbH, Schiedlberg, Austria). All electrodes were filled with highly conductive gel in order to reduce impedance. Participants were free to move their eyes during the recordings, but were instructed to reduce all unnecessary muscular activity.

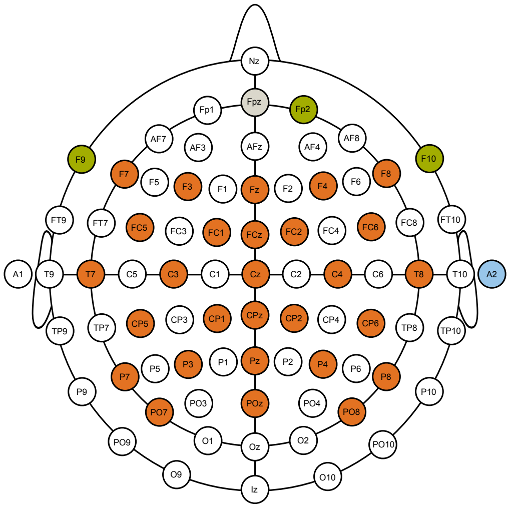

Figure 1: EEG/EOG electrode placement.

3.3. Experimental paradigms

In the present study, three different experimental paradigms (to be explained in the following subsections) were designed to investigate *interaction* ErrPs. Participants were required to complete one experiment per visit and therefore they visited the laboratory on three separate occasions spaced few days apart. Half of the participants did Exp. II, I and III on the first, second and third visit/day, respectively. The other half did the experiments in the order III, I and II. Additionally, in order to examine the invariance and variability of ErrPs over time, some participants were invited to revisit the lab for additional times, where they repeated experiments they have already completed in the first three visits/days. These participants ended up doing the same experiment twice on separate days. Subject S1 repeated the second experiment three times. We will refer to different recordings of the same experiment as the *1st, 2nd and 3rd recordings* for these subjects. Each experiment consisted of multiple sessions, where each session lasted around 11 min. Since it is important to maintain a high attention level during task operation, breaks were given between sessions and subjects were free to stop a recording session at any time. Each experiment lasted for around 2 hours, including the preparation and break times. Break times were paced by individual subjects and were overall in the range 1-15 min. Consequently, the number of recorded

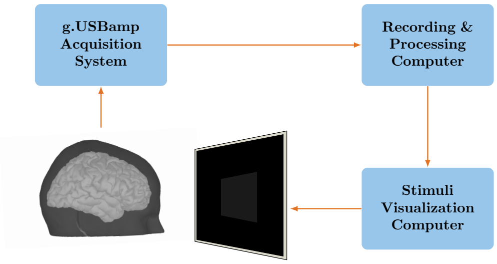
g.USBamp Acquisition System
Recording & Processing Computer
Stimuli Visualization Computer

Figure 2: System overview showing the main modules. Recording and stimulation were done on the same machine for Exp. I. Visual stimuli were presented on a 60 Hz LCD monitor.

sessions and trials varied across subjects.

In all experiments, participants were instructed to mentally evaluate the interface actions as correct or erroneous. Figure 2 shows the main modules used for the experimental setup in all three experiments, where the acquisition of the data and offline processing were facilitated with Simulink/MATLAB software (MathWorks, Massachusetts, United States). The experimental design for each of the experiments is described in the following subsections, and a summary that relates the respective tasks and explains the reasons behind their choice will be presented in subsection 3.3.4.

3.3.1. Experiment I: Keyboard-mediated ball game task

Very similar to [12], participants were instructed to use the left and the right arrow keyboard keys in order to move a ball towards a hole (respectively the sphere and the rectangle in figure 3), where both were aligned to the same horizontal line at the middle of the display. Each game run started with the ball randomly placed 5 steps away from the hole, either to the right or to the left with equal probabilities. In this work, we refer to all trials that are recorded while the hole is being to the right of the ball as *right trials* and otherwise as *left trials*. Following each key press issued by the participant, the ball moved one step in the direction of the pressed key with a probability of 80% and in the opposite direction with the remaining probability. In order to isolate motor-related potentials due to key presses from potentials following the feedback presentation, the ball appeared in the new location τ s after each key press, where τ is uniformly drawn in the interval $[0.9, 1.1]$ s. Immediately after key presses, the color of the ball turned from green into red, indicating that further key presses will be ignored and the ball remained red for a period of 2 s. Subjects were instructed not to try to interact with the ball during this time. Once the ball reached the hole, a new game run was started after 2 s. Each subject finished multiple sessions and depending on the individual interaction pace, each session consisted of a varying number of runs and consequently a varying number of ErrP/noErrP trials.

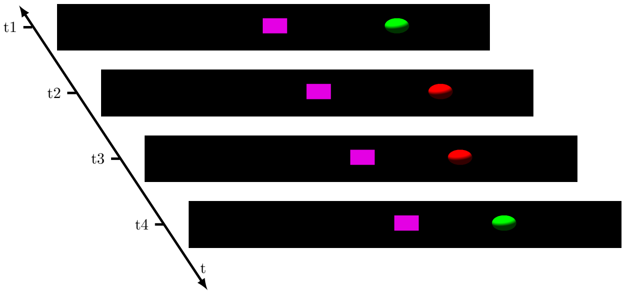

Figure 3: Key events in the keyboard-based interaction experiment. At time t_1, the user presses the key which brings the ball towards the hole (left key in the shown case). In the next display frame, the ball turns red and stays in place for a duration randomly drawn from the interval $[0.9, 1.1]$ s. Afterwards at t_3, the ball moves one step either to the right or the left according to user input and the error random generation. The ball remains inactive (red) after this movement till t_4. Shown is the correct case here and therefore EEG data time-locked to t_3 is considered a correct trial (noErrP). Note that $t_4 - t_1 = 2$ s.

3.3.2. Experiment II: P300-based interaction with central feedback

A P300 training session was first performed in copy spelling row-column flashing mode using a 6x6 spelling matrix containing the alphanumerals. This session, which lasted around 4 minutes, started with one character briefly highlighted in green on the P300 matrix. Participants were instructed to attend to the cued character during the flashing sequence that followed and consisted of 16 repetitions. In a single repetition, all rows and columns were flashed in a random order, where in each flashing, a row or a column was highlighted on the screen for 100 ms and the time between the onset of two consecutive flashes was set to 183.34 ms. Following the end of the complete flashing sequence, a different character was highlighted in green, followed by another complete flashing sequence. This procedure was repeated till 5 characters were cued, each followed by a complete flashing sequence. As such, during this session, participants did not actively produce any spelled character.

An LDA classifier was learned from this training session and used to estimate the hidden user intentions in the following online P300 sessions. In order to facilitate the acquisition of ErrP and noErrP training examples in the online P300 sessions, we have designed a simple mathematical task, wherein participants were instructed to attend to the maximum number in a 5x5 P300 matrix (example is shown in figure 4). The P300 matrix in every new trial was filled with new random numbers, generated so all of them except one, were either 1 or 2-digit numbers. The remaining number, which was the maximum, consisted of 3 digits. Participants were informed about the fact that only one number consisted of 3 digits. This renders the mathematical task very simple or rather reduced to a simple visual search task, where the possibility a user makes a mistake by him/herself is minimized. Every ErrP/noErrP trial started with a new set of numbers randomly drawn and distributed within the P300 matrix, so that the location of the target maximum number was changed with every new trial. The update of the P300 matrix was facilitated by the XML interface described in [54]. In order to collect as many labeled ErrP and noErrP trials as possible, the flashing sequence in each trial was restricted in most cases to two repetitions. The accuracy of spelling, however, was monitored throughout the different sessions and the number of repetitions was sometimes modified to keep a relatively balanced number of ErrP and noErrP trials for each subject. Precisely, when a subject made many errors during a specific session, the number of repetitions per trial was increased in subsequent sessions so that the error rate could be reduced. In contrast, the number of repetitions was reduced following low error rates. The number of repetitions was never below 2 and error rates in the range 40-60% did not imply any change in the used number of repetitions.

After a decision was made about the user intent in the online P300 sessions, flashing was stopped and the mask was completely emptied for a duration of one second. Then, an empty square was shown at the center of the display for one second, aiming at directing the user's gaze to this location [30]. The estimated user intent (number) was shown afterwards inside the square for another second. The time between the end of the last flash and the presentation of the estimated number was therefore 2 seconds. Figure 4(a) shows the key events in a single ErrP/noErrP trial. Each subject underwent a different number of sessions, each consisted of a different number of ErrP/noErrP trials.

It is noteworthy here that the P300 training and online sessions differ with respect to the task (spelling vs. finding maximum number) and the matrix size (6x6 vs. 5x5). Hereby, the straightforward classifier transfer across these sessions confirms previous findings that P300-based BCIs generalize across different operational tasks [39, 41, 55, 56], and across different matrix sizes [57].

3.3.3. Experiment III: P300-based interaction with inplace feedback

This experiment shared all details of Exp. II except the way the feedback was shown to users. Hereby, the mask remained displayed after flashing was stopped for 2 s and the estimated number was then highlighted for 1 s with a red square as shown in figure 4(b). After highlighting the estimated number, the P300 matrix was updated with a new set of random numbers.

3.3.4. Interrelation among experiments

Exp. II and III differ only with respect to the style of feedback presentation. On the one hand, should the central method be used for feedback presentations as in Exp. II, subjects need to test whether the presented number is a 3-digit number or not. On the other hand, to assess the correctness of interface actions in case of Exp. III, no comparison is necessary, as noticing that the visual feedback is shown on the P300 matrix over a place that does not match the previously attended one is sufficient to realize that an error has occurred. Thus, the feedback presentation in erroneous trials in this case is expected to be the target of a rapid eye movement (i.e. saccade). About 200 ms [58] are typically required for the eye to make such a movement. For correct trials, the feedback is shown overlaid on the previously fixated number, and therefore no saccades are expected to take place. It can be argued for Exp. III, therefore, that the processing of the feedback stimuli in case of erroneous trials starts at a later point in time compared to correct ones.

Obviously, the two feedback strategies in Exp. II and III require different mental processes to arrive at a decision whether the estimated number is correct or not. As such, these two experiments in particular enable us to examine invariance/variability of *interaction* ErrPs during P300-mediated interaction with respect to the required mental processing.

The reasons we chose the maximum number task in these experiments are threefold. Firstly, this task requires no memorization of the last attended letter at the time of feedback onset as it is the case in spelling P300 applications with central feedback, which may reduce the effects of mind wandering and attentional lapses [59]. Secondly, the task allows to collect ErrP/noErrP trials without relying on copy spelling and sham feedback modes, allowing for better resemblance of P300-based online interaction. Thirdly, with the continuous updating of the P300 matrix, the task simulates the case of interacting with an adaptive P300 interface, which updates its contents based on the current context in a dynamic environment. Such adaptivity can be of high importance to enable enhanced interaction in robotic BCI applications [56].

Exp. I differs from both Exp. II and III with

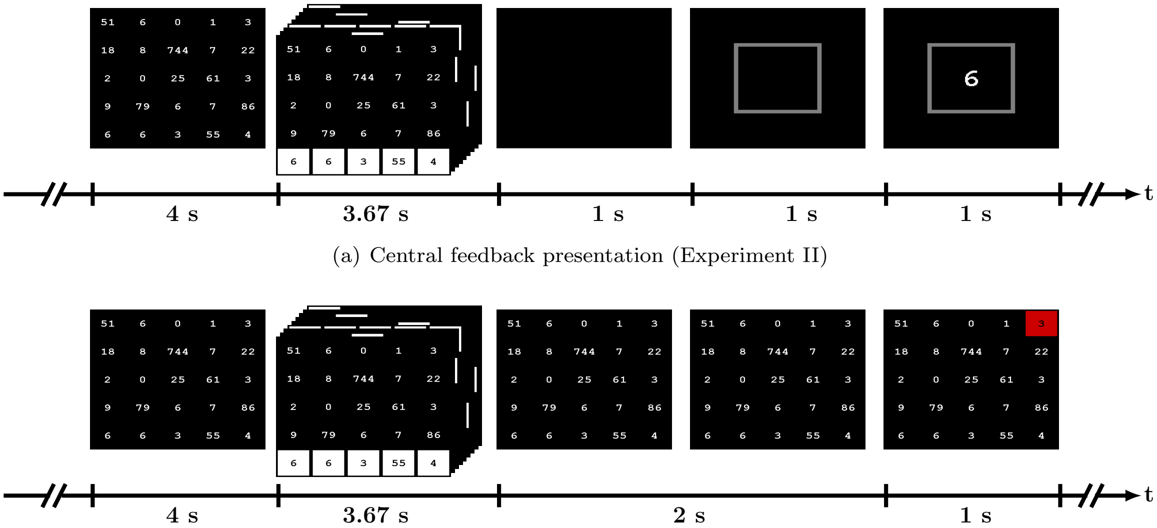

(a) Central feedback presentation (Experiment II)

(b) Inplace feedback presentation (Experiment III)

Figure 4: Key events in experiments II and III. The flashing time (3.67 s) is shown as an example for the case when two flashing repetitions were used.

respect to the user input (keyboard vs. P300), where we also introduced about 1 s delay between the user input and the feedback onset in Exp. I and 2 s in Exp. II and III. The 1 s delay in Exp. I and the 2 s delay in Exp. II are sufficient to respectively isolate hand-movement and eye-movement-related potentials. The 2 s delay in Exp. III was chosen to match that of Exp. II. Supported by the remarks from subsection 2.2, the main difference in our understanding between the different experiments, is the mental processing required to assess the movement of the ball in Exp. I compared to the processing of the central and inplace feedback in the P300-based interaction experiments. Furthermore, the presence of EOG artifacts that accompany feedback onset in Exp. I will be useful to understand the effect of these artifacts in Exp. I and III.

3.4. Classification

Two binary classification problems are encountered within this work with the goal of discriminating between target and nontarget flashes (in Exp. II and III) and between single trial ErrP and noErrP (in all experiments). In both cases, the goal is to find a mapping function $h : \mathcal{X} \rightarrow \mathcal{Y}$, that maps from the domain of the d-dimensional feature space $\mathcal{X} = \mathbb{R}^d$ to the range of class labels $\mathcal{Y} = \{\omega_1, \omega_2\}$.

In supervised classification methods, h is learned from a training dataset ($\mathcal{D}$) containing $n = n_1 + n_2$ tuples of observations and their labels, i.e.
$\mathcal{D} = \{(\mathbf{x}^{(1)}, h(\mathbf{x}^{(1)})), (\mathbf{x}^{(2)}, h(\mathbf{x}^{(2)})), \cdots (\mathbf{x}^{(n)}, h(\mathbf{x}^{(n)}))\}$, where $h(\mathbf{x}^{(i)})) \in \{\omega_1, \omega_2\} \ \forall i$, and n_1 and n_2 are the number of available examples for class ω_1 and ω_2, respectively. LDA assumes two normal distributions for the two classes, such that $\mathbf{x}|\omega_1 \sim \mathcal{N}(\boldsymbol{\mu}_1, \boldsymbol{\Sigma}_1), \mathbf{x}|\omega_2 \sim \mathcal{N}(\boldsymbol{\mu}_2, \boldsymbol{\Sigma}_2)$, and that the two classes share a common covariance matrix (i.e. $\boldsymbol{\Sigma}_1 = \boldsymbol{\Sigma}_2 = \boldsymbol{\Sigma}$). The LDA-based mapping function can be computed with $h_{LDA} = \text{sign}(\mathbf{w}^T\mathbf{x} + b)$, where $\mathbf{w}$ and b to be learned from $\mathcal{D}$ with class labels mapped to $\omega_1 = 1$, $\omega_2 = -1$. The weighting vector can be computed with $\mathbf{w} = \boldsymbol{\Sigma}^{-1}(\boldsymbol{\mu}_1 - \boldsymbol{\mu}_2)$ and the bias with $b = \frac{-1}{2}(\boldsymbol{\mu}_1 + \boldsymbol{\mu}_2)^T\mathbf{w}$.

Since the true means and covariance matrices for each class are unknown, estimates thereof are substituted for the computations of $\mathbf{w}$ and b. The sample means are computed with $\hat{\boldsymbol{\mu}}_1 = \frac{1}{n_1}\sum_{i=1}^{i=n_1}\mathbf{x}^{(i)}$ and $\hat{\boldsymbol{\mu}}_2 = \frac{1}{n_2}\sum_{i=n_1+1}^{i=n}\mathbf{x}^{(i)}$, and the pooled sample covariance matrix is computed with
$\hat{\boldsymbol{\Sigma}} = \frac{1}{n-2}\left[(n_1 - 1)\hat{\boldsymbol{\Sigma}}_1 + (n_2 - 1)\hat{\boldsymbol{\Sigma}}_2\right]$, where $\hat{\boldsymbol{\Sigma}}_1$ and $\hat{\boldsymbol{\Sigma}}_2$ are the within-class sample covariance matrices, which can be estimated with
$\hat{\boldsymbol{\Sigma}}_1 = \frac{1}{n_1-1}\sum_{i=1}^{i=n_1}(\mathbf{x}^{(i)} - \hat{\boldsymbol{\mu}}_1)(\mathbf{x}^{(i)} - \hat{\boldsymbol{\mu}}_1)^T$ and similarly for $\hat{\boldsymbol{\Sigma}}_2$. These estimates of the covariance matrices are known as the maximum likelihood (ML) estimates, which fail to provide invertible $\hat{\boldsymbol{\Sigma}}$ when $n < d$ [60]. As a remedy in such situations, we adopted the analytical shrinkage covariance estimator proposed in [60] (using function `cov_shrink()` from BCILAB [61]). Throughout this paper, we will refer to the LDA with ML covariance estimator as ML-LDA and with the shrinkage estimator as shrinkage-

LDA. The former is used to classify P300 trials (since $n_1, n_2 > d$) and the latter is used to classify ErrP trials (as fewer number of trials were acquired especially for Exp. II and III).

3.5. Pre-processing and feature extraction pipeline

Pre-processing and feature extraction of P300 and ErrPs differ fundamentally as a result of differences in their spatial, temporal and spectral characteristics. The P300 pipeline used here is based on previous works [62, 63] that have shown good classification/spelling accuracies with LDA classifiers, and was decided upon before our recordings took place to facilitate discriminating target and nontarget trials in online P300 sessions. The ErrP pipeline was, on the other hand, adopted post hoc to facilitate our offline analysis.

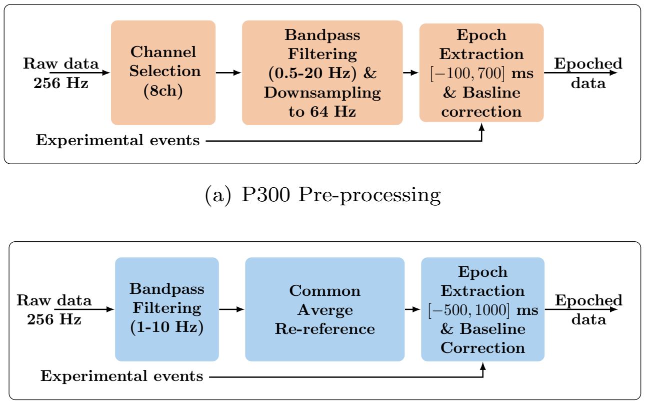
Raw data
256 Hz
Channel Selection (8ch)
Bandpass Filtering (0.5-20 Hz) & Downsampling to 64 Hz
Epoch Extraction $[-100, 700]$ ms & Basline correction
Epoched data
Experimental events
Raw data
256 Hz
Bandpass Filtering (1-10 Hz)
Common Averge Re-reference
Epoch Extraction $[-500, 1000]$ ms & Baseline Correction
Epoched data
Experimental events

(a) P300 Pre-processing

(b) ErrP Pre-processing

Figure 5: The different pre-processing and epoch extraction pipelines for P300 and ErrP. Feature extraction is performed on the epoched data.

3.5.1. P300 pre-processing and feature extraction Only a subset of the EEG electrodes (Fz, Cz, P3, Pz, P4, PO7, POz and PO8) were used for P300 classification during experiments II and III, since P300 is believed to have a central and parietal distribution. Additionally, EEG data from these electrodes were shown to lead to relatively good P300 classification accuracies [64]. The continuous raw data from these 8 electrodes were notch-filtered at 50 Hz, bandpass-filtered with a 4^{th} order butterworth filter in the range $0.5 - 20$ Hz (since P300 is believed to be composed of phase-locked delta, theta and alpha oscillations [65–68]) and downsampled to 64 Hz.

Event-locked EEG epochs of 800 ms duration were extracted from the pre-processed continuous data about the onset of each target/nontarget flash, i.e. a baseline of 100 ms pre-stimulus and 700 ms post-stimulus. The temporal mean of the baseline at each electrode was then subtracted from the post-stimulus data. A schematic of this pre-processing pipeline is depicted in figure 5(a).

Features per electrode were obtained by downsampling the epoched data with a factor of 3, and features from the 8 electrodes were finally concatenated to form the labeled feature vectors (with a resulting dimensionality of $8 \times \lceil 0.7 \times 64/3 \rceil = 120$). Each training session produced respectively around 160 and 800 target and nontarget training trials, which were used to train an ML-LDA classifier. In online sessions, feature vectors were obtained with the same pre-processing and feature extraction pipeline, where the unknown label of each feature vector was estimated with the learned ML-LDA classifier. Noteworthy here is that we did not aim at optimizing the accuracy of the P300-based interaction during the performed experiments (e.g. by using shrinkage-LDA to classify target/nontarget flashes [37] or by optimizing the number of repetitions), but rather at collecting as many ErrP and noErrP single trials as possible, with a reasonable number of flashing repetitions.

3.5.2. ErrP pre-processing and feature extraction The continuous EEG data from all 28 electrodes were first bandpass-filtered with a 4^{th} order butterworth filter in the range $1 - 10$ Hz (since ErrP is believed to be relatively slow cortical potentials [12, 42, 69]) and then re-referenced to the common spatial average (i.e. the spatial mean was subtracted from each channel) to enhance SNR. EEG epochs in the period $[-0.5, 1.0]$ s time-locked to the feedback onset were extracted from the pre-processed EEG data and corrected for the 500 ms pre-stimulus baseline (i.e. the temporal mean of the baseline data was subtracted from the post-stimulus data). This pipeline is schematically shown in figure 5(b).

Features per electrode were obtained by downsampling the epoched data by a factor of 8. Feature vectors were then obtained by concatenating features in the time region $[0.15, 1]$ s following the feedback onset from the 5 midline electrodes (Fz, FCz, Cz, CPz and Pz), resulting in a dimensionality of $5 \times \lfloor 0.85 \times 256/8 \rfloor = 135$. Hereby, the selection of the midline channels is supported by the fact that ErrPs exhibit a fronto-central distribution along the midline [12] and that features from the central brain regions result in superior classification accuracy when compared to the peripheral regions [51].

3.6. Analysis of interaction ErrP invariance and variability

3.6.1. Neurophysiological analysis: The average correct and error potentials were computed per subject from EEG epochs of 1.5 s duration extracted about the feedback onset consisting of 0.5 s pre-stimulus and 1 s post-stimulus data. We base our analysis hereby mainly on the grand EEG average (i.e. the average over subjects) of the correct and error trials, to which we will refer respectively as the GAC, GAE. The grand average difference waveform (i.e. GAD) is simply the difference between GAE and GAC. All waveforms will be shown for either the frontocentral electrode FCz or the vertex (i.e. Cz), since several studies have pointed out a strong role of the ACC and adjacent frontocentral brain areas in monitoring errors [70].

Epochs, which contained, within the first post-stimulus second, EEG potentials outside the range $\pm 50\mu$V or EOG potentials outside the range $\pm 200\mu$V were excluded from the average computation, aiming at preventing strong ocular (e.g. eye blinks) artifacts from appearing in the average signals.

Statistical analysis of the difference between GAE and GAC signals within each experiment is performed using the adaptive factor adjustment procedure described in [71], controlling for the false discovery rate (FDR) at the 0.05 level. To this end, the function `erpfatest` from R `ERP` package is used.

Additionally, the signed r^2 discriminability test [41, 72] is performed on correct and error trials of each subject in order to highlight the major spatial and temporal sources of variance among them within the different experiments. Intuitively, the unsigned r^2 quantifies the proportion of the total amplitude variance that is explained by the ground truth labels of the acquired sample data. Formally, it is computed for a certain feature with

$$r_k^2 = \frac{\operatorname{cov}(\mathbf{x}_k, \boldsymbol{\omega})^2}{\operatorname{var}(\mathbf{x}_k)\operatorname{var}(\boldsymbol{\omega})}, \tag{1}$$

where the vector $\boldsymbol{\omega}$ is constructed from all the sample labels, i.e. $\boldsymbol{\omega} = [h(\mathbf{x}^{(1)}), h(\mathbf{x}^{(2)}), \cdots h(\mathbf{x}^{(n)})]^T$ and $\mathbf{x}_k$ is constructed by concatenating the k^{th} element of the d-dimensional feature vectors. The signed r^2 is computed with $r^2 \cdot \operatorname{sign}(\operatorname{cov}(\mathbf{x}_k, \boldsymbol{\omega}))$. Similar to [11], r^2 is used to assess the signal-to-noise ratio (SNR) of the different ErrP peaks.

3.6.2. ErrP classification: A 10-fold cross-validation was used to evaluate the performance of the shrinkage-LDA classifier in predicting the correct (noErrP) and incorrect (ErrP) trials obtained during the different experiments. In order to better estimate the classification accuracy in online sessions, all extracted trials, including the ones with strong ocular artifacts, were used for the classifier training and testing. Accuracy is reported in terms of the *true positive rate* (TPR or sensitivity) and *true negative rate* (TNR or specificity), which respectively reflect the rate of correct decoding of erroneous and correct trials. The different experimental tasks produce imbalanced data sets (i.e. numbers of ErrP and noErrP trials are different), typically resulting in biased classification towards the majority class [51]. As a remedy, the normalized mutual information (NMI) [2] was additionally adopted as a single metric that incorporates both sensitivity and specificity. The reader is referred to [2] for the exact definition of NMI and its computation procedure, but it is important to note that NMI lies between 0 and 1, with the values 0 and 1, respectively reflecting chance-level (i.e. no class structure is found by the classifier) and perfect classification accuracy.

Furthermore, in order to quantify the invariance in ErrPs with respect to the different experimental factors (subjects, time and mental processes required to assess interface actions), the accuracy of classifier transfer across the different levels of these factors are reported. In particular, with respect to subjects, we choose to use per-experiment leave-one-subject-out cross validation method, where data from all subjects but one are used to train a classifier, which is then applied on the data of the left-out subject. The procedure is repeated separately for each experiment. On the other hand, with respect to time, we choose to use per-experiment and per-subject cross-day validation method, where the data from a specific subject/recording is used to test a classifier that is trained using data acquired from a previous recording of the same experiment. Finally, with respect to the mental processing, per-subject leave-one-experiment-in cross validation [73] is used. Hereby, the data from each experiment is used to train a classifier which is then applied on the data from each other experiment. This procedure is repeated for each subject.

In order to assess the significance of the obtained accuracies (quantified with NMI), p-values were obtained using the label randomization test procedure [74], where 1000 permutations were performed in total. P-values below 0.05 are considered to be statistically significant, i.e. rejecting the null hypothesis that the data and class labels are independent, that is, there is no difference between the classes [74].

4. Experimental results

4.1. Datasets

Table 1 provides a summary of the total number of trials and the number of error trials collected for each subject/experiment/recording. On average, 13.4% trials were labeled as noisy and were excluded from the computation of the GAE, GAC and GAD. However, in the different contexts of classification in this work, all recorded trials were used.

Table 1: Number of extracted trials written in the form (Number of ErrP trials/Total number of trials). Percentage of ErrP to total trials is shown in parentheses.

Subject	Exp. I	Exp. II	Exp. III
S1	274/1315 (20.8%)	68/149 (45.6%)	62/125 (49.6%)
S1 (2nd rec.)		174/341 (51.0%)	162/309 (52.4%)
S1 (3rd rec.)		174/338 (51.5%)	
S2	228/1099 (20.7%)	71/149 (47.7%)	77/191 (40.3%)
S3	273/1382 (19.8%)	64/139 (46.0%)	111/186 (59.7%)
S3 (2nd rec.)			156/326 (47.9%)
S4	337/1664 (20.3%)	164/245 (66.9%)	85/147 (57.8%)
S4 (2nd rec.)	313/1408 (22.2%)		178/333 (53.5%)
S5	262/1381 (19.0%)	135/215 (62.8%)	152/248 (61.3%)
S5 (2nd rec.)			184/302 (60.9%)
S6	340/1675 (20.3%)	124/191 (64.9%)	119/190 (62.6%)
S7	277/1432 (19.3%)	81/250 (32.4%)	88/278 (31.7%)
S7 (2nd rec.)		66/286 (23.1%)	
S8	285/1539 (18.5%)	174/295 (59.0%)	122/289 (42.2%)
S9	327/1532 (21.3%)	194/294 (66.0%)	190/313 (60.7%)
S10	307/1611 (19.1%)	212/331 (64.0%)	241/323 (74.6%)

4.2. Neurophysiological analysis

4.2.1. Experiment I: The GAC, GAE and GAD for Exp. I are shown in figure 6(a). The GAD exhibits an early positivity around 220 ms (P2), early negativity around 280 ms (N2) followed by a positivity around 340 ms (P3) and a later wider negativity around 460 ms (N4). Following the adaptive factor adjustment procedure [71], the difference was found to be significant around all the observed peaks except for the N2. Visual inspection of the GAE and GAC waveforms reveals that the P3 and N4 deflections are specific to error trials. The SNR value and the peak latency of these GAD peaks for each subject/recording are reported in table 2.

Furthermore, since the correct direction of the ball movement in Exp. I was randomly alternating between the right and the left direction with each new run, correct and incorrect trials for these two conditions obviously result in different HEOG traces. This can be seen in figure 7, where the average HEOG traces were plotted separately for the right and left trials alongside the GAC, GAE and GAD waveforms. Hereby, all average waveforms are computed by averaging an equal number of left and right trials for each subject. The observed discrepancy in the HEOG traces, did not propagate to the electrode site FCz, as one can hardly observe any difference in the GAC, GAE, GAD waveforms computed separately for the two directions. These results are in agreement with [12] and find support in [75], where it is argued that horizontal eye movement have no effect on the central sites.

4.2.2. Experiment II: The GAD waveform at FCz, plotted in figure 6(b), is characterized with a negative peak (N) at around 330 ms and a later positive peak (P) at around 430 ms. Visual inspection of the GAC and GAE waveforms reveals that these two deflections are particularly present in error trials. Further, the time regions around these peaks are identified to be statistically significant following the adaptive factor adjustment procedure [71]. Per subject SNR and peak latency of the two peaks are presented in table 2.

4.2.3. Experiment III: The GAD waveform at FCz, plotted in figure 6(c), is characterized by a negative peak (N) at around 260 ms and a later positive peak (P) at around 380 ms. The peak amplitudes and latencies of the two peaks are reported for each subject/recording in table 2. Visual inspection of the GAE and GAC shows that both waveforms are characterized with a positivity and a later negativity. A Wilcoxon paired rank sum test ($p = 0.064$) revealed a trend toward a difference in the latency of the positivity between the GAE and GAC. This difference is estimated to be around 0.05 s and might be attributed to the extra time required to notice the flash on the screen in case of error trials. As such, this delay is likely to be, as well, the source of the two deflections in the GAD waveform.

Arguably, the activity at the FCz site in case of errors after t = 0 cannot be explained by the ocular artifacts (or saccades) that accompany these errors, since similar activity, yet with a different peak latency, is observed in correct trials where no eye movement is required.

4.3. Within-experiments Classification Results

The 10-fold cross-validation classification accuracies for each subject/experiment/recording are shown in table 3. The classification sensitivity and specificity are estimated to be respectively around 74% and 80% on average, which is comparable with results reported in similar *interaction* ErrPs studies with different classifiers (e.g. sensitivity and specificity around 82% and 83% with a Gaussian classifier [12], average accuracy around 80% using a support vector machine (SVM) classifier [30] and around 77% using neural networks [51]). The NMI metric is estimated to be around 25%, 30% and 39% for Exp. I, II and III, respectively. The permutation test revealed that all obtained accuracies are significant (meaning that these accuracies are obtained from classifiers that have found a significant class structure for the respective individual/experiment/recording), except for subject S5 in Exp. II, for whom both the negativity and the positivity were found to have low SNR levels as listed in table 2. Overall, the obtained results reiterate the significant difference between the correct and error trials within each experiment, allowing to train significant classifiers that are specific for individuals/experiments/recordings.

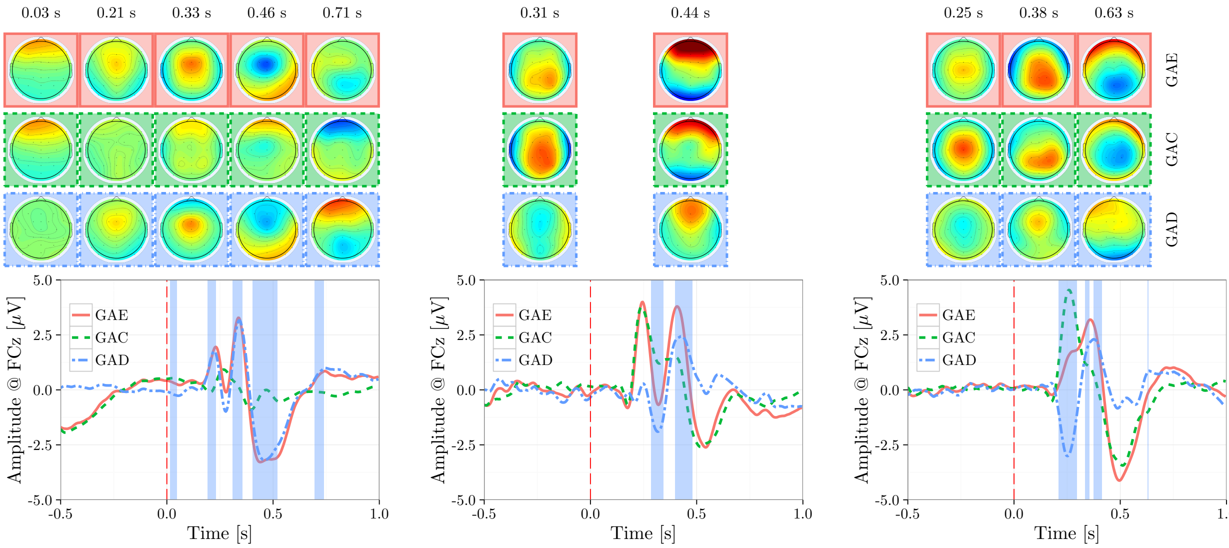

(a) Experiment I

(b) Experiment II

(c) Experiment III

Figure 6: The GAC, GAE and GAD waveforms were computed from the average of all subjects and recordings for all experiments. The shaded areas represent significant time regions in GAD as identified with the adaptive factor adjustment procedure described in [71]. Scalp topographies of voltage amplitudes (averaged over the significant time regions) are plotted in the upper panel.

Table 2: Per-subject SNR (r^2) and latency values for the different peaks of the GAD waveform in the three experiments. Shaded rows highlight the second and third recordings of subjects who perfomed one experiment (or more) mutliple times. The coefficient of variation (CV) of each column is tabulated in the last row.

	Experiment I				Experiment II				Experiment III			
	P3		N4		N		P		N		P	
Subject	SNR (r^2)	Latency	SNR (r^2)	Latency	SNR (r^2)	Latency	SNR (r^2)	Latency	SNR (r^2)	Latency	SNR (r^2)	Latency
S1	0.259	0.36	0.157	0.46	0.289	0.31	0.230	0.39	0.251	0.27	0.208	0.35
S1 (2nd rec.)					0.057	0.31	0.131	0.38	0.234	0.25	0.058	0.37
S1 (3rd rec.)					0.073	0.32	0.096	0.38				
S2	0.218	0.34	0.182	0.44	0.039	0.33	0.084	0.43	0.058	0.25	0.241	0.37
S3	0.037	0.34	0.029	0.42	0.159	0.30	0.252	0.39	0.420	0.25	0.263	0.39
S3 (2nd rec.)									0.277	0.25	0.167	0.38
S4	0.003	0.39	0.007	0.52	0.190	0.35	0.206	0.46	0.231	0.25	0.163	0.40
S4 (2nd rec.)	0.007	0.33	0.009	0.57					0.154	0.25	0.087	0.40
S5	0.091	0.37	0.049	0.47	0.010	0.37	0.013	0.50	0.039	0.24	0.002	0.37
S5 (2nd rec.)									0.048	0.25	0.029	0.35
S6	0.013	0.32	0.135	0.44	0.021	0.34	0.173	0.54	0.009	0.26	0.081	0.42
S7	0.029	0.36	0.057	0.45	0.015	0.32	0.101	0.40	0.089	0.30	0.109	0.38
S7 (2nd rec.)					0.051	0.32	0.204	0.38				
S8	0.074	0.34	0.064	0.43	0.099	0.35	0.159	0.45	0.131	0.27	0.027	0.34
S9	0.086	0.35	0.087	0.49	0.050	0.34	0.112	0.47	0.153	0.27	0.007	0.33
S10	0.308	0.34	0.256	0.45	0.016	0.29	0.009	0.39	0.050	0.27	0.103	0.43
mean± std	**0.102 ± 0.11**	**0.35±0.02**	**0.094±0.08**	**0.47±0.04**	**0.082±0.08**	**0.33±0.02**	**0.136±0.08**	**0.43±0.05**	**0.153±0.12**	**0.26±0.01**	**0.110±0.09**	**0.38±0.03**
CV	**1.06**	**0.06**	**0.85**	**0.10**	**1.01**	**0.07**	**0.56**	**0.12**	**0.76**	**0.06**	**0.78**	**0.08**

4.4. Invariance and variability in ErrPs with respect to subjects

Figure 8 shows per-subject average difference waveform separately for each experiment. The variability across subjects is also shown with the shaded area, representing the standard error of the mean. From these plots and the results in table 2, one can observe inter-subject variability with respect to the amplitudes and SNR of the different deflections. The timing of the different deflections, however, seems to be more consistent across subjects as indicated by the values of the coefficient of variation (i.e., the standard deviation divided by the mean) reported in the last row of table 2. As in [51], it can be argued that the high variance of classification accuracy across subjects, reported in table 3, can be attributed to the fact that these subjects have different concentration levels on the performed tasks.

Furthermore, table 4 lists, separately for each experiment, the leave-one-subject-out cross validation accuracies for the classifier transfer. The permutation test indicated that the obtained accuracies are significant (meaning that these accuracies are obtained from classifiers that have found a significant class structure for the respective ErrP/noErrP dataset) for

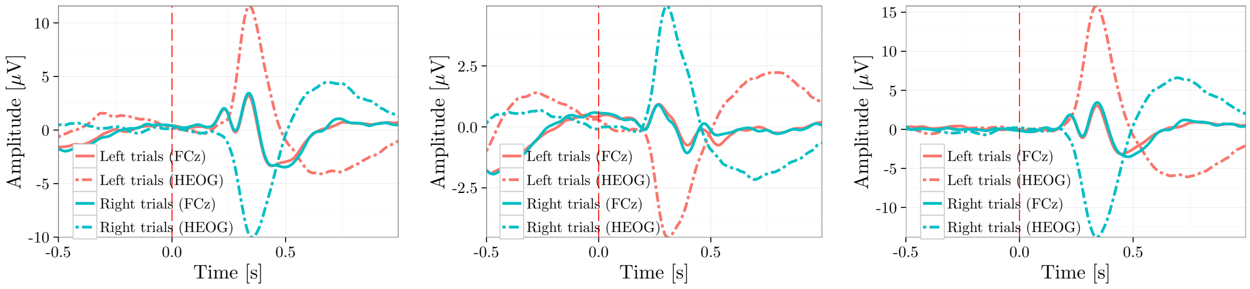

(a) GAE (b) GAC (c) GAD

Figure 7: The GAE, GAC and GAD waveforms computed from equivalent number of left and right trials per subject in Exp. I at the electrode site FCz and for HEOG.

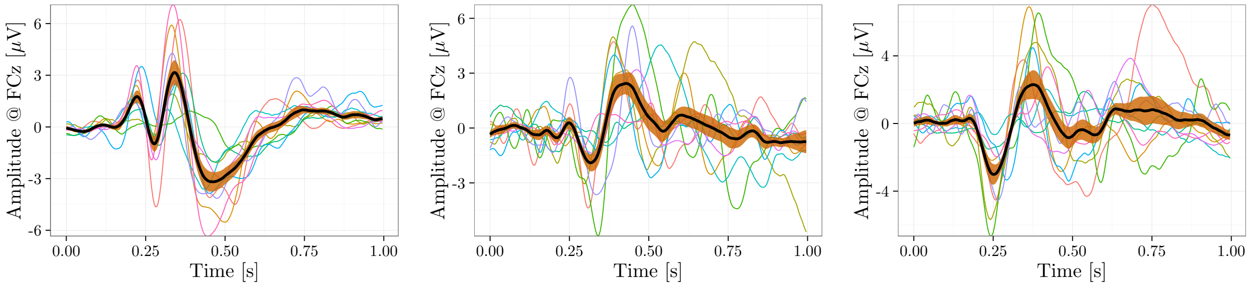

(a) Experiment I (b) Experiment II (c) Experiment III

Figure 8: The average difference (error-minus-correct) waveform plotted for each subject in Exp. (a) I, (b) II and (c) III. Shaded area represents the standard error estimate across the different subjects.

all subjects Exp. I and 70% of all subjects in Exp. II and III. However, it can be easily seen that the obtained NMI values are inferior to the cross-validation accuracies obtained for each subject/experiment listed in table 3. The differences were observed to be 0.09, 0.2 and 0.22, respectively for Exp. I, II and III. These differences were revealed to be significant with Wilcoxon paired rank sum tests, applied separately for each experiment on the data tabulated in table 3 and table 4, and corrected for multiple tests using the Benjamini-Hochberg false discovery rate control procedure [76]. Corrected p-values were ($p = 0.002$) for all experiments.

Altogether, these results suggest that despite inter-subject variability that negatively affects classifier transfer performance, invariant features across subjects can be obtained.

4.5. Invariance and variability in ErrPs over time

Figure 9 shows the GAD waveforms computed for the participants S4, S1 and S3 who completed multiple recordings for experiments I, II and III, respectively. Visual inspection of these plots shows that the shapes of the ErrPs are empirically invariant over time for the same experiment/interface/subject. This observation which is valid for all our three interfaces agrees with [12], where the same is shown using an interface very similar to the one in Exp. I. Combined with the results in table 2, it can be observed that the SNR, amplitude and latency of the different peaks are quite stable over time.

Furthermore, table 5 lists the NMI values obtained for the shrinkage-LDA trained with data of one recording, and applied on data from a later recording of the same subject/experiment. The table only shows the results for the subjects who have multiple recordings for the same experiment. The permutation test indicated that the classifier transfer accuracy is significant (meaning that these accuracies are obtained from classifiers that have found a significant class structure for the respective ErrP/noErrP dataset) for all subjects. However, it can be easily seen that the NMI experiences a reduction of 0.13 on average compared to the values from table 3, which is revealed to be significant with a Wilcoxon paired rank sum test ($p = 0.004$). Nonetheless, the classification results altogether reemphasize our belief that ErrPs are empirically invariant to a larger extent over time

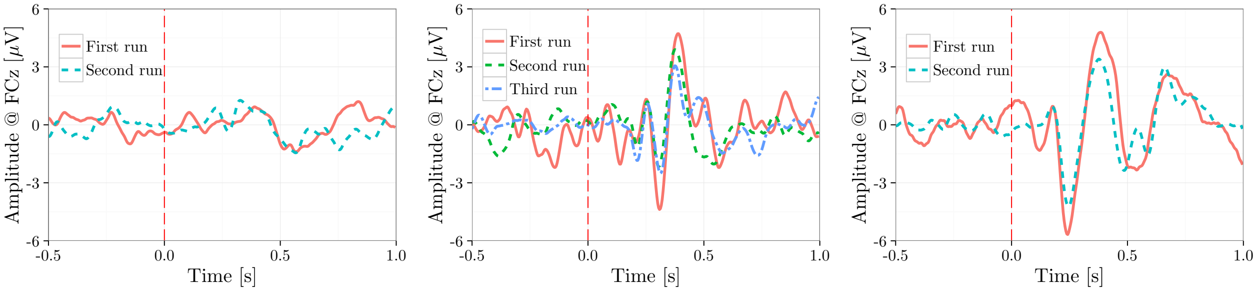

(a) Experiment I (b) Experiment II (c) Experiment III

Figure 9: Examples of the GAD waveforms computed for the different experiments for some subjects who performed one experiment or more on multiple occasions.

than over subjects for the same experiment/interface, which is also supported by the similar GAD waveforms obtained for the different days.

4.6. Invariance/variability with respect to human mental processing of interface actions

In section 4.2, we have compared the GAE and GAC waveforms to reason about the observed components in the GAD waveform for each experiment. In the following, we compare the GAE and GAC waveforms across experiments to reason about the variability/invariance in the computed GAD waveforms with respect to the mental processing required to assess the interface actions. To this end, figure 10 rearranges the GAE, GAC and GAD waveforms from figure 6 and plots them over experiments.

4.6.1. Experiment II vs. III

As can be seen from figure 10(c) and table 2, both the GAD waveforms of Exp. II and III are characterized by a negativity and a later positivity. Further, from figure 6 and other results in section 4.2 ,we have seen that not only the timing of the two deflections varied across experiments, but also their relation to the time course of the GAC and GAE waveforms. In Exp. II, the two ErrP deflections in the GAD were primarily present in error trials, whereas in Exp. III, the deflections might have appeared as a result of the time delay in processing the error trials relative to the correct ones. The different mental processes required to evaluate the interface actions, as has been discussed in 3.3.4, might provide a plausible explanation to this variability. It can be seen from figures 10 and 11 that the difference in the GAE waveforms across experiments is larger than that in the GAC waveforms. This additionally might hint at a role of the mental processing in the observed variability.

4.6.2. Experiment I vs. II

The discrepancy in the GAD waveform between Exp. I and Exp. II has been already observed in the literature, e.g. Spüler and Niethammer note that the first positive peak and the N4 is not visible in interaction ErrPs for all BCI tasks [42]. In the current work, and by analyzing figure 6, we have additionally seen that the P3 and N4 deflections in the GAD waveform of Exp. I and the N and P deflections of Exp. II stem from their particular presence in error trials.

4.6.3. Per-subject across-experiments classifier transfer

The classification accuracies for the classifier transfer across the different experiments are listed in table 6. These results show that the classifier transfer between Exp. I and II, and between Exp. I and III provide insignificant and low accuracies for most subjects. The accuracies of the classifier transfer between Exp. II and III show significant results for almost half of the subjects.

5. Discussion

5.1. Significance of the results

The present study addressed between and within-subject sources of invariance/variability in interaction ErrP and showed a strong evidence that some invariant features exist across the different subjects and over time, replicating previous conclusions in this respect. On the other hand, convergent evidence has been obtained suggesting that different mental processes required to assess interface actions give rise to distinguishable ErrP waveforms. The same has also been confirmed with a low across-experiments generalizability of the LDA classifier, especially between Exp. I on one hand, and Exp. II and III on the other hand. The accuracies of the classifier transfer between Exp. II and III show

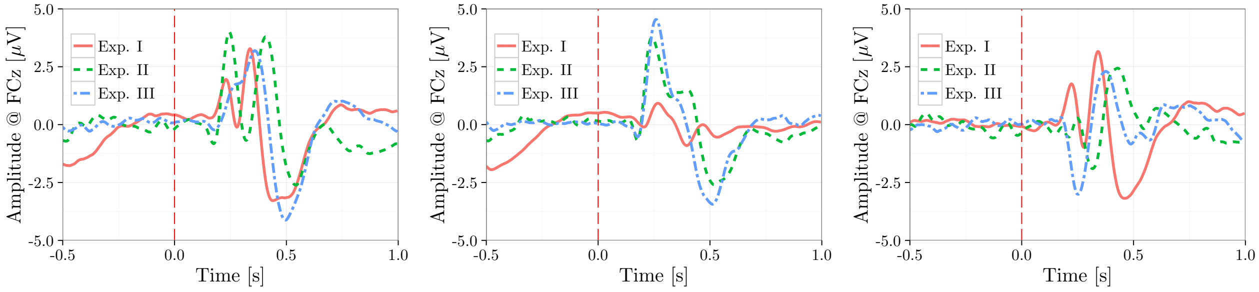

(a) GAE (b) GAC (c) GAD

Figure 10: The GAE, GAC and GAD waveforms for the three experiments.

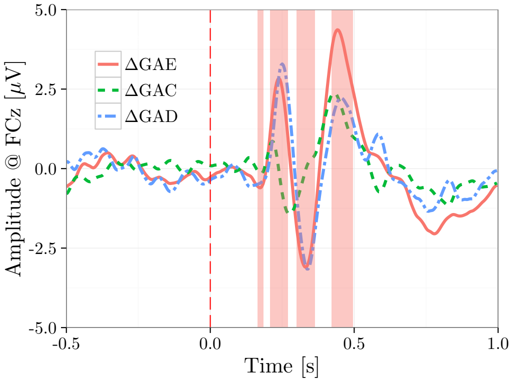

Figure 11: The difference in GAE, GAC and GAD waveforms across Exp. II and III.

significant results for almost half of the subjects, where the results also show that the rate of correct detection of correct trials (TNR) is higher than that of incorrect trials (TPR). The later observation suggests that the similarity of the GAC waveforms in both experiments (i.e., II and III) may have contributed to these results.

Furthermore, the relative invariance of ErrPs over time, and the identical pre-processing pipeline used for all experiments rule out their possible involvement in producing the observed variability across the different experiments. Conversely, it can be argued that should there be a considerable difference in the shape of the grand average error and correct trials across experiments/studies with the same tasks, different mental processes are expected to underly this difference. It cannot be said with certainty, however, that the observed variability in ErrPs can be fully accounted for by these factors. Variables like the structure/modality of the feedback, the pre-processing pipeline, the rarity/frequency of error occurrences [12], the severity of the error (i.e., the degree of mismatch between the actual outcome and user expectation) [77] and possible ocular and muscular artifacts may contribute as well to such variations, and such contribution should be reduced as much as the experimental paradigms might allow.

Our results emphasize that different ErrP studies and the results obtained therefrom should be carefully compared, and a similarity in the GAD waveform should be always confirmed with respect to the separate averages of error and correct trials. For instance, the apparent similar shapes of the GAD waveforms in Exp. II and III might hint at a mere difference in latency between the peaks of the two signals. The larger signal difference in GAE between the experiments, as can be seen in figure 11, may rule out such explanation and instead, suggests a role of the different mental processing of the feedback stimuli. Furthermore, visual inspection of the average waveforms in Exp. II and III reveals the presence of the N4 component in both GAC and GAE waveforms, which was clearly absent in the GAD waveforms. Therefore, it would have been certainly misleading to just show the similarity of GAD waveforms in experiments II and III, or to claim that the late N4 component is specific to Exp. I.

In this work, we have investigated the invariance/variance of ErrPs mainly at the FCz electrode. Furthermore, despite the fact that ErrPs can be evaluated in both the spectral and temporal domains, the focus of this study was laid upon the temporal domain and therefore no claim whatsoever about the spectral variability is made. Some evidence exists in the literature, however, suggesting that the spectral responses to errors may vary as well with respect to different types of errors, e.g. between *execution* and *outcome* errors [42].

5.2. *Comparison with relevant studies*

It is generally challenging to compare the results of different studies as there are several sources of variability involved. In order to illustrate this, in the following we try to highlight the similarities/differences between the GAD waveforms from our experiments to

Table 3: 10-fold cross-validation classification accuracy. Accuracy is reported in terms of TPR, TNR and NMI. All results were significant except for subject S5 in Exp. II.

Subject	Metric	Exp. I	Exp. II	Exp. III
S1	TPR	0.75 ± 0.07	0.88 ± 0.09	0.79 ± 0.13
	TNR	0.95 ± 0.02	0.80 ± 0.11	0.78 ± 0.19
	NMI	0.43 ± 0.09	0.43 ± 0.19	0.32 ± 0.20
S2	TPR	0.79 ± 0.06	0.79 ± 0.15	0.83 ± 0.18
	TNR	0.95 ± 0.02	0.86 ± 0.08	0.88 ± 0.12
	NMI	0.48 ± 0.10	0.39 ± 0.27	0.49 ± 0.23
S3	TPR	0.60 ± 0.12	0.89 ± 0.11	0.90 ± 0.05
	TNR	0.73 ± 0.04	0.85 ± 0.14	0.89 ± 0.08
	NMI	0.08 ± 0.06	0.52 ± 0.24	0.56 ± 0.18
S4	TPR	0.57 ± 0.08	0.91 ± 0.06	0.89 ± 0.10
	TNR	0.68 ± 0.05	0.88 ± 0.12	0.86 ± 0.14
	NMI	0.05 ± 0.03	0.57 ± 0.22	0.55 ± 0.31
S5	TPR	0.65 ± 0.09	0.57 ± 0.17	0.61 ± 0.15
	TNR	0.81 ± 0.03	0.47 ± 0.18	0.59 ± 0.18
	NMI	0.15 ± 0.05	0.05 ± 0.06	0.06 ± 0.09
S6	TPR	0.71 ± 0.09	0.82 ± 0.06	0.67 ± 0.08
	TNR	0.90 ± 0.02	0.75 ± 0.20	0.66 ± 0.18
	NMI	0.31 ± 0.09	0.30 ± 0.20	0.11 ± 0.10
S7	TPR	0.71 ± 0.08	0.68 ± 0.17	0.85 ± 0.14
	TNR	0.80 ± 0.03	0.79 ± 0.07	0.95 ± 0.05
	NMI	0.19 ± 0.06	0.18 ± 0.09	0.61 ± 0.19
S8	TPR	0.79 ± 0.06	0.75 ± 0.10	0.83 ± 0.13
	TNR	0.90 ± 0.01	0.72 ± 0.16	0.87 ± 0.11
	NMI	0.38 ± 0.06	0.19 ± 0.10	0.47 ± 0.22
S9	TPR	0.66 ± 0.09	0.73 ± 0.09	0.90 ± 0.04
	TNR	0.81 ± 0.03	0.64 ± 0.08	0.87 ± 0.12
	NMI	0.17 ± 0.06	0.11 ± 0.08	0.52 ± 0.12
S10	TPR	0.79 ± 0.07	0.75 ± 0.10	0.79 ± 0.08
	TNR	0.95 ± 0.02	0.60 ± 0.17	0.68 ± 0.21
	NMI	0.48 ± 0.09	0.11 ± 0.10	0.20 ± 0.14
S1 (2nd rec.)	TPR		0.69 ± 0.10	0.85 ± 0.06
	TNR		0.70 ± 0.13	0.81 ± 0.07
	NMI		0.14 ± 0.09	0.36 ± 0.14
S1 (3rd rec.)	TPR		0.86 ± 0.10	
	TNR		0.78 ± 0.15	
	NMI		0.37 ± 0.17	
S3 (2nd rec.)	TPR			0.85 ± 0.08
	TNR			0.88 ± 0.06
	NMI			0.46 ± 0.14
S4 (2nd rec.)	TPR	0.58 ± 0.11		0.90 ± 0.06
	TNR	0.68 ± 0.05		0.89 ± 0.04
	NMI	0.05 ± 0.04		0.53 ± 0.13
S5 (2nd rec.)	TPR			0.70 ± 0.11
	TNR			0.70 ± 0.23
	NMI			0.16 ± 0.11
S7 (2nd rec.)	TPR		0.73 ± 0.13	
	TNR		0.93 ± 0.06	
	NMI		0.42 ± 0.19	
mean	TPR	**0.69± 0.09**	**0.77± 0.10**	**0.81± 0.09**
	TNR	**0.83± 0.10**	**0.75± 0.13**	**0.81± 0.11**
	NMI	**0.25± 0.17**	**0.29± 0.17**	**0.39± 0.18**

Table 4: Leave-one-subject-out cross validation accuracies for each subject. Accuracies were significant except for the cells highlighted in orange.

	Experiment I			Experiment II			Experiment III		
Sub.	ErrP	noErrP	NMI	ErrP	noErrP	NMI	ErrP	noErrP	NMI
S1	0.79	0.84	0.28	0.84	0.51	0.09	0.85	0.37	0.04
S2	0.82	0.84	0.32	0.87	0.53	0.13	0.77	0.75	0.19
S3	0.48	0.80	0.06	0.61	0.91	0.22	0.80	0.89	0.38
S4	0.44	0.75	0.03	0.63	0.88	0.20	0.82	0.68	0.19
S5	0.38	0.87	0.06	0.50	0.53	0.00	0.57	0.53	0.00
S6	0.38	0.95	0.14	0.81	0.27	0.00	0.93	0.15	0.01
S7	0.78	0.51	0.06	0.65	0.66	0.07	0.74	0.90	0.33
S8	0.80	0.70	0.16	0.65	0.73	0.10	0.54	0.86	0.13
S9	0.51	0.90	0.15	0.77	0.49	0.05	0.93	0.67	0.32
S10	0.83	0.85	0.33	0.54	0.58	0.01	0.80	0.49	0.07
mean	**0.62**	**0.80**	**0.16**	**0.69**	**0.61**	**0.09**	**0.78**	**0.63**	**0.17**

Table 5: Classification accuracies computed for the classifier transfer over time (NMI_t) compared to the 10-fold cross validation NMI values from table 3. All results were identified as significant by the permutation test. The time gap (in days) between the different recordings is listed under Δd.

Exp.	Sub.	Train w/	Test w/	Δd	NMI	NMI_t
I	S4	1st rec.	2nd rec.	3	0.05 ± 0.04	0.04
II	S1	1st rec.	2nd rec.	33	0.14 ± 0.09	0.13
	S1	1st rec.	3rd rec.	38	0.37 ± 0.17	0.18
	S1	2nd rec.	3rd rec.	5	0.37 ± 0.17	0.19
	S7	1st rec.	2nd rec.	6	0.42 ± 0.19	0.30
III	S1	1st rec.	2nd rec.	17	0.36 ± 0.14	0.15
	S3	1st rec.	2nd rec.	30	0.46 ± 0.14	0.43
	S4	1st rec.	2nd rec.	47	0.53 ± 0.13	0.25
	S5	1st rec.	2nd rec.	14	0.16 ± 0.11	0.06
				mean	**0.32**	**0.19**

the results from relevant studies in the literature. In particular, the interfaces in Exp. I and Exp. II have been previously used in the literature, and similar GAD waveform have been reported. Fig 12(a) compares the GAD obtained for Exp. I (solid line) and that in [12] (sparsely dashed line). We observe that the two waveforms exhibit high similarity with respect to their general shape, yet with a considerable variability with respect to the observed peak amplitudes and latencies. The shift in P3 latency was found to be significant; $t(9) = 5.38, p < 0.001$. Additionally, the waveform of the *execution error* in [42] is plotted on the same figure (sparsely dotted line), where similar observation about the peak amplitudes and latencies can be made as before. Since there is a great similarity in the nature of the erroneous actions across these studies (the interface deliberately moves a virtual object in directions that mismatch the user input), it may be argued that this variability is due to between-subject variations. Further, the different pre-processing pipelines used to produce these results might have made a contribution. To support the last argument, we have examined the effect of two simple modifications to our pre-processing pipeline. The first modification (M1) consists of removing the common average re-reference block from

Table 6: Per-subject leave-one-experiment-in cross validation accuracy. All NMI values were not significant except for the shaded cells.

	Exp. I						Exp. II						Exp. III					
	Exp. II			Exp. III			Exp. I			Exp. III			Exp. I			Exp. II		
Sub.	ErrP	noErrP	NMI	ErrP	noErrP	NMI	ErrP	noErrP	NMI	ErrP	noErrP	NMI	ErrP	noErrP	NMI	ErrP	noErrP	NMI
S1	0.18	0.96	0.03	0.64	0.79	0.14	0.62	0.31	0.00	0.42	0.69	0.01	0.61	0.69	0.06	0.23	0.74	0.00
S2	0.03	0.91	0.00	0.45	0.68	0.01	0.11	0.77	0.02	0.56	0.89	0.18	0.36	0.77	0.01	0.66	0.79	0.15
S3	0.61	0.35	0.00	0.89	0.09	0.00	0.38	0.48	0.00	0.37	0.83	0.03	0.63	0.43	0.00	0.52	0.87	0.12
S4	0.56	0.48	0.00	0.89	0.36	0.06	0.72	0.28	0.00	0.49	0.78	0.06	0.70	0.42	0.00	0.51	0.70	0.03
S5	0.15	0.82	0.00	0.40	0.60	0.00	0.48	0.36	0.00	0.46	0.41	0.00	0.53	0.45	0.00	0.30	0.65	0.00
S6	0.10	0.91	0.00	0.61	0.45	0.00	0.81	0.28	0.00	0.75	0.48	0.04	0.54	0.35	0.00	0.71	0.55	0.05
S7	0.77	0.50	0.05	0.89	0.33	0.04	0.43	0.71	0.01	0.74	0.83	0.24	0.62	0.54	0.02	0.57	0.81	0.11
S8	0.15	0.80	0.00	0.57	0.62	0.02	0.48	0.29	0.00	0.48	0.26	0.00	0.64	0.54	0.02	0.16	0.79	0.00
S9	0.39	0.59	0.00	0.56	0.60	0.02	0.72	0.24	0.00	0.69	0.45	0.01	0.86	0.20	0.00	0.36	0.65	0.00
S10	0.10	0.90	0.00	0.37	0.71	0.00	0.58	0.29	0.00	0.68	0.59	0.04	0.57	0.31	0.00	0.60	0.57	0.02
mean	**0.30**	**0.72**	**0.01**	**0.63**	**0.52**	**0.03**	**0.53**	**0.40**	**0.00**	**0.56**	**0.62**	**0.06**	**0.61**	**0.47**	**0.01**	**0.46**	**0.71**	**0.05**

the original pipeline shown in figure 5(b), whereas in the second (M2), the EEG epochs are extracted directly from the raw data and linearly detrended by removing the best straight-line that fits the data of each electrode. The GAD waveforms resulting from using M1 (densely dotted line) and M2 (densely dashed line) with the data of Exp. I are additionally plotted on figure 12(a). The new GAD plots obviously show that the way the data is pre-processed affects the latency and amplitude of the observed peaks, where spatial mean subtraction reduces the amplitude of the observed deflections (as can be seen by comparing the results of M1 and the original pipeline) and the temporal filtering additionally introduces time shifts in the data (as can be seen by comparing the results of M2 and the original pipeline).

Similarly, the GAD waveform for Exp. II is plotted alongside those from [30, 44] in figure 12(b). Again, the between subject variations and the different processing pipeline might have contributed to the observed variability. Herein, however, one cannot rule out the contribution of the different mental processing to these discrepancies, as the maximum number and the language spelling tasks could have required different mental processing of the interface actions.

5.3. The effect of the error rarity/frequency

It has been already established that the error rate has an impact on the observed amplitude (but not the time course) of the ErrP signals [12]. More specifically, it has been shown that a rare error (with frequency 20%) leads to larger amplitudes when compared to more frequent errors (with frequency 50%) [12]. The amplitude difference may be attributed according to [12] to possible contributions of the Oddball N2 and P3 in case of error rates of 20%. Therefore, the discrepancy in our experiments regarding error rates, might have also contributed to why subject-specific classifiers could not be transferred between Exp. I (where error rates were targeted to be around 20%) on one hand and Exp. II and III (where error rates were targeted to be around 50%) on the other hand. However, should it be true, that the mismatch in error rates gave rise to the large variability between experiments, then for classifier transferability to work eventually across experimental paradigms, one needs to control for the error rates among these experiments.

5.4. ErrPs Invariance at electrodes other than FCz

This work has mainly investigated the invariance/variability of ErrPs measured at the FCz electrode location. This channel has been chosen primarily as the areas to its underneath are repeatedly shown to be involved in responding to observed/committed errors. As such, the invariance/variability reported here, is practically a manifestation of the invariance/variability of how these areas respond to errors. Conversely, and depending on the exact model of the head volume conduction, EEG measured at any electrode placed at the scalp may also capture the activity of these areas, and if so, this activity should be subject to the same invariance/variability factors as the activity recorded at FCz. This leads us to argue that the obtained results regarding the invariance of ErrPs at FCz, can be generalized (but with caution) to other electrode locations that capture the error monitoring and processing activities in the brain. Electrodes, that are placed at locations that do not capture the error-related activity, should manifest no difference between error and correct trials, and should manifest great invariance in this regard. However, these arguments need to be verified with future work.

5.5. The effect of the classifier choice

Throughout this work, we have assumed the existence of invariant temporal ErrP features with respect to a specific factor on the basis of classifier generalizability across its different levels. The LDA classifier was chosen for classification since its results can be

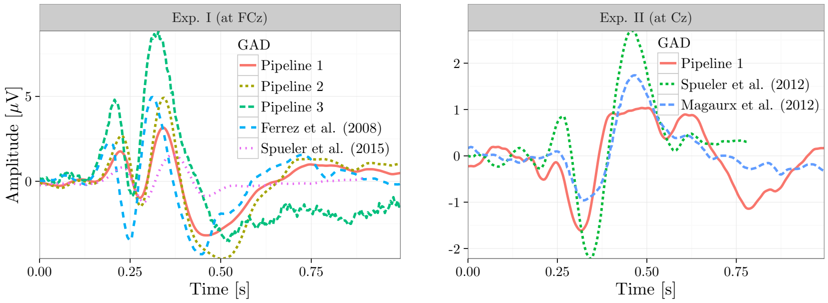

(a) Experiment I

(b) Experiment II

Figure 12: Comparison of the obtained GAD waveforms with reported averages in the literature. (a) The GAD waveform at electrode FCz obtained with Exp. I is compared to the GAD reported in [12, 42]. There is a considerable shift between the two signals, but the shape remains very similar. The GAD is also shown when computed using *Pipeline 1* and *2*. (b) The GAD waveform at Cz obtained from the data of Exp. II, compared to the GAD in [30, 44].

interpreted by referring to the first and second moments of the (temporal) ErrP/noErrP distributions. Obviously, other classifiers, e.g. SVM or neural networks, may result in different results, but such results may not be easily interpreted. Generally speaking, the LDA classifier finds the optimal 1-dimensional subspace, on which the projected values of the sample feature vectors have maximal correlation with their labels. Optimality is guaranteed when the sample data of the two classes are drawn from normal distributions with different means ($\boldsymbol{\mu}_1 \neq \boldsymbol{\mu}_2$) and a common covariance matrix $\boldsymbol{\Sigma}$. The LDA optimal subspace is obtained directly from the means and the covariance matrix as was described in subsection 3.4. Since the GAD waveforms (i.e. $\boldsymbol{\mu}_1 - \boldsymbol{\mu}_2$) of the different experiments were found to be stable over time, it is reasonable to think that the reduced performance of the transferred LDA classifier over time stems from the fluctuations in the covariance matrix.

Furthermore, the differences observed in GAD, GAE and GAC waveforms across experiments, suggest that one needs to at least recalibrate trained classifiers for the means of the new interfaces, which requires to acquire new training examples. The effectiveness of LDA recalibration with respect to the new mean values has been already confirmed in [41]. The applicability of this approach is additionally supported by the results in [78] where it is shown that error-related brain activity can be assessed on the basis of 6-8 trials only. Further, with prolonged usage of BCIs as in [79], training examples of ErrP/noErrP can be obtained alternatively in retrospect from the rich previous history of interaction by exploiting the structure of the interface to label post-feedback EEG epochs as erroneous/correct [32, 80].

5.6. Impact on P300-ErrP BCIs

The current work shows the ability of supervised LDA classification to decode *interaction* ErrPs for both the inplace and central feedback strategies, yet the former has shown better cross validation results and better across-subject classifier transferability. Based on the major results of this work, we hypothesize that the inplace feedback has another favorable aspect. That is, the ErrP in inplace feedback strategy is independent of the task, for which P300-based interaction is used, whereas in case of central feedback, different mental processes may be required to assess interface actions for different tasks. For instance, in spelling applications, feedback stimuli are assessed based on the correctness of the spelled characters, whereas in maximum number task, judging the correctness of the feedback involves judging whether the presented number consists of 3 digits or not. The validation of this hypothesis is left to future work. Furthermore, ErrP classification has been treated throughout this work as a supervised classification problem. That is mainly due to the nature of P300-based interaction tasks presented. In sequential tasks (as the ball game of Exp. I in this work) with feedback signals, unsupervised ErrP classification has been shown to achieve good results [81].

5.7. Interrelations with other types of ErrP

In this work, our main focus was laid upon the *interaction* ErrPs and their variability/invariance. Yet, the results obtained hereby find support in studies of other types of ErrPs as has been already reported in section 2 regarding relevant results for *observation* ErrPs.

Furthermore, in speeded choice RT tasks like flanker task, *observation* ErrPs are characterized with ERN that peak at around 250 ms. This negativity is similar to that in response ErrPs, yet with longer latency and reduced amplitude, suggesting that similar neural mechanisms are involved in assessing performed and observed actions [5]. Along this vein, the experiments in [82] investigated *observation* ErrPs in a VR environment where users observed avatars performing reach-to-grasp actions from first-person perspective (1PP) and third-person perspective (3PP). It has been found that observation of erroneous actions in 1PP enhances the ERN, Pe and spectral theta and alpha bands powers compared to 3PP, suggesting that the action monitoring system is maximally activated for ones own errors and when others errors are coded as if they were as such. Similarily, feedback ErrPs were reported to have a negativity peaking in the time range [200-300] ms following externally generated errors (i.e. malfunctions) in speeded choice RT tasks [23]. According to authors, the different latencies of ERN in the different types of ErrPs indicate a possibility of being dependent on the source of information about goal achievement rather than about the performance itself [23], where self-generated errors are recognized more rapidly compared to externally generated errors, as for the latter case, feedback stimuli need to go through the sensory system first. This is also consistent with the results of [8], where it was shown that the latency and peak amplitude of feedback negativity are sensitive with respect to the used feedback modality and to stimulus discriminability. Other factors like the response-set size [83], the perceived accuracy of actions [25], and whether accurate performance or response speed is emphasized [69], have a strong effect on the ERN and CRN observed with subjects performing different versions of flanker task.

Together, these results converge to suggest that a similarity in the mental processing of committed/observed errors give rise to variability that affects the amplitude and latency of the different peaks/components in ErrPs. On the contrary, differences in the general shape of ErrPs across experiments/studies suggests the recruiting of different mental processes therein.

5.8. The effect of user tiredness

Tiredness is a major source of nonstationarity in the brain, typically giving rise to strong alpha rhythms in EEG signals [35]. We conjecture that tiredness has affected all our experimental conditions and subjects equally, and no particular observation made here can be directly connected to user tiredness.

6. Conclusion

Using three different noisy interfaces, this paper has examined the invariance vs. variability of *interaction* ErrPs with respect to: (1) the mental processes required to assess interface actions (2) time (3) subjects. By fixing the pre-processing pipeline for all experiments, we have shown that the *interaction* ErrPs for each experiment enjoyed invariance to some extent across subjects and over time. This invariance in turn resulted in a relative robustness of the shrinkage-LDA classifier across subjects and over time. On the other hand, we have shown that the mental processes which are required to assess interface actions highly affect the observed *interaction* ErrPs. This has been supported by the differences in the observed GAC, GAE and GAD waveforms across interfaces/experiments. The observed variability with respect to the respective mental processes has also been shown to make it difficult for a classifier learned from the data of one experiment/interface to straightforwardly transfer to other experiments/interfaces. In particular, despite the similarity of the GAD waveforms in experiments II and III, where subjects performed exactly the same task but with different feedback presentation methods, shrinkage-LDA classifier which was learned from data of one experiment showed low accuracies for most subjects when tested on data from the other interface. Again, this proves the sensitivity of the ErrPs to the nature of the mental processing of correct and incorrect interface actions, which takes place immediately after the feedback onset.

In this work, we didn't try to compare the many existing advanced spatial and spatio-temporal filtering methods that enhance the SNR or the ErrPs. But using simple alteration of the pre-processing pipeline, we have shown that great variability can be introduced with respect to the timing and amplitude of the different components of *interaction* ErrPs.

In summary, the variability in the different interaction ErrP studies (including ours) was found largely attributable to the different mental processing required to assess interface actions. Conversely, given two interfaces which require the exact same mental processing after feedback onset in correct and incorrect trials, our results suggest that any discrepancy with respect to the amplitude and latency of the different ErrP components are most likely caused by inter-subject variability, the non-stationarity of the EEG data or differences in the pre-processing pipeline. These discrepancies propagate as well to the classification step and affects the obtained accuracies.

Acknowledgments

This work is supported in part by the VERE project within the 7th Framework Programme of the European Union, FET-Human Computer Confluence Initiative, contract number ICT-2010-257695 and the Institute of Advanced Study of the Technical University of Munich (TUM).

References

[1] Alex Kreilinger, Christa Neuper, and Gernot R. Müller-Putz. Error potential detection during continuous movement of an artificial arm controlled by brain-computer interface. *Medical and Biological Engineering and Computing*, 50(3):223–230, 2012.

[2] Tomislav Milekovic, Tonio Ball, Andreas Schulze-Bonhage, Ad Aertsen, and Carsten Mehring. Detection of Error Related Neuronal Responses Recorded by Electrocorticography in Humans during Continuous Movements. *PLoS ONE*, 8(2), 2013.

[3] M. Falkenstein, J. Hohnsbein, J. Hoormann, and L. Blanke. Effects of crossmodal divided attention on late ERP components. II. Error processing in choice reaction tasks. *Electroencephalography and clinical neurophysiology*, 78(6):447–455, 1991.

[4] Gert-Jan Munneke, Tanja S. Nap, Eveline E. Schippers, and Michael X Cohen. A statistical comparison of EEG time- and time-frequency-domain representations of error processing. *Brain Research*, 1618:222–230, 2015.

[5] Hein T van Schie, Rogier B Mars, Michael G H Coles, and Harold Bekkering. Modulation of activity in medial frontal and motor cortices during error observation. *Nature neuroscience*, 7(5):549–54, may 2004.

[6] Wolfgang H. R. Miltner, Jens Brauer, Holger Hecht, Ralf Trippe, and Michael G. H. Coles. Parallel brain activity for self-generated and observed errors. In *Errors, conflicts, and the brain: current opinions on performance monitoring*, pages 124–129. Leipzig: Max Planck Institute for Human Cognitive and Brain Sciences., 2004.

[7] Su Kyoung Kim and Elsa Andrea Kirchner. Handling Few Training Data: Classifier Transfer between Different Types of Error-Related Potentials. *IEEE Transactions on Neural Systems and Rehabilitation Engineering*, 24(3):320–332, 2016.

[8] Wolfgang H. R. Miltner, Christoph H. Braun, and Michael G. H. Coles. Event-related brain potentials following incorrect feedback in a time-estimation task: Evidence for a ”generic” neural system for error detection. *Journal of cognitive neuroscience*, 9(6):788–798, 1997.

[9] Nick Yeung, Clay B. Holroyd, and Jonathan D. Cohen. ERP correlates of feedback and reward processing in the presence and absence of response choice. *Cerebral Cortex*, 15(5):535–544, 2005.

[10] Marco Congedo, Sandra Rousseau, and Christian Jutten. An Introduction to EEG Source Analysis with an Illustration of a Study on Error-Related Potentials. In Eduardo Reck Miranda and Julien Castet, editors, *Guide to Brain-Computer Music Interfacing*, pages 163–189. Springer, 2014.

[11] Gerwin Schalk, Jonathan R. Wolpaw, Dennis J. McFarland, and Gert Pfurtscheller. EEG-based communication: presence of an error potential. *Clinical neurophysiology*, 111(12):2138–2144, dec 2000.

[12] Pierre W. Ferrez and José Del R. Millán. Error-related EEG potentials generated during simulated brain-computer interaction. *IEEE transactions on biomedical engineering*, 55(3):923–929, mar 2008.

[13] Michael Falkenstein, Jörg Hoormann, Stefan Christ, and Joachim Hohnsbein. ERP components on reaction errors and their functional significance: a tutorial. *Biological psychology*, 51(2):87–107, jan 2000.

[14] Tanja Endrass, Julia Klawohn, Julia Preuss, and Norbert Kathmann. Temporospatial dissociation of Pe subcomponents for perceived and unperceived errors. *Frontiers in human neuroscience*, 6:178, 2012.

[15] Elke Godefroid, Gilles Pourtois, and Jan R. Wiersema. Joint effects of sensory feedback and interoceptive awareness on conscious error detection: Evidence from event related brain potentials. *Biological Psychology*, 114:49–60, 2016.

[16] Phan Luu, Don M. Tucker, and Scott Makeig. Frontal midline theta and the error-related negativity: Neurophysiological mechanisms of action regulation. *Clinical Neurophysiology*, 115(8):1821–1835, 2004.

[17] Cameron S. Carter, Todd S. Braver, Deanna M. Barch, Mathhew M. Botvinick, Douglas Noll, and Johathan D. Cohen. Anterior cingulate cortex, error detection, and the online monitoring of performance. *Science*, 280(5364):747–749, may 1998.

[18] Daniel H. Mathalon, Susan L. Whitfield, and Judith M. Ford. Anatomy of an error: ERP and fMRI. *Biological Psychology*, 64(1-2):119–141, 2003.

[19] William J. Gehring, Yanni Liu, Joseph M. Orr, and Joshua Carp. The Error-Related Negativity (ERN/Ne). In Steven J. Luck and Emily S. Kappenman, editors, *The Oxford Handbook of Event-Related Potential Components*. Oxford University Press (UK), 2012.

[20] Thomas Michelet, Bernard Bioulac, Dominique Guehl, Michel Goillandeau, and Pierre Burbaud. Single medial prefrontal neurons cope with error. *PLoS ONE*, 4(7):0–5, 2009.

[21] David C Godlove, Erik E Emeric, Courtney M Segovis, Michelle S Young, Jeffrey D Schall, and Geoffrey F Woodman. Event-related potentials elicited by errors during the stop-signal task. I. Macaque monkeys. *The Journal of neuroscience : the official journal of the Society for Neuroscience*, 31(44):15640–9, 2011.

[22] Jessica M. Phillips and Stefan Everling. Event-related potentials associated with performance monitoring in non-human primates. *NeuroImage*, 97:308–320, 2014.

[23] Antje Gentsch, Peter Ullsperger, and Markus Ullsperger. Dissociable medial frontal negativities from a common monitoring system for self- and externally caused failure of goal achievement. *NeuroImage*, 47(4):2023–2030, 2009.

[24] Jacob B. Hirsh and Michael Inzlicht. Error-related negativity predicts academic performance. *Psychophysiology*, 47(1):192–196, 2010.

[25] Martin K. Scheffers and Michael G. H. Coles. Performance monitoring in a confusing world: error-related brain activity, judgments of response accuracy, and types of errors. *Journal of experimental psychology. Human perception and performance*, 26(1):141–151, 2000.

[26] Joseph T Gwin, Klaus Gramann, Scott Makeig, and Daniel P Ferris. Removal of movement artifact from high-density EEG recorded during walking and running. *Journal of Neurophysiology*, 103(6):3526–34, 2010.

[27] Carrie A. Joyce, Irina F. Gorodnitsky, and Marta Kutas. Automatic removal of eye movement and blink artifacts from EEG data using blind component separation. *Psychophysiology*, 41(2):313–325, 2004.

[28] Jonathan R. Wolpaw, Herbert Ramoser, Dennis J. McFarland, and Gert Pfurtscheller. EEG-based communication: improved accuracy by response verification. *IEEE transactions on rehabilitation engineering*, 6(3):326–333, sep 1998.

[29] Adrien Combaz, Nikolay Chumerin, Nikolay V. Manyakov, Arne Robben, Johan A. K. Suykens, and Marc M. Van Hulle. Towards the detection of error-related potentials

and its integration in the context of a P300 speller brain-computer interface. *Neurocomputing*, 80:73–82, 2012.

[30] Martin Spüler, Michael Bensch, Sonja Kleih, Wolfgang Rosenstiel, Martin Bogdan, and Andrea Kübler. Online use of error-related potentials in healthy users and people with severe motor impairment increases performance of a P300-BCI. *Clinical Neurophysiology*, 123(7):1328–1337, jul 2012.

[31] Timothy Zeyl, Erwei Yin, Michelle Keightley, and Tom Chau. Improving bit rate in an auditory BCI: Exploiting error-related potentials. *Brain-Computer Interfaces*, 3(2), 2016.

[32] Nico M. Schmidt, Benjamin Blankertz, and Matthias S. Treder. Online detection of error-related potentials boosts the performance of mental typewriters. *BMC Neuroscience*, 13(1):1, 2012.

[33] Alex Kreilinger, Hannah Hiebel, and Gernot R. Muller-Putz. Single Versus Multiple Events Error Potential Detection in a BCI-Controlled Car Game with Continuous and Discrete Feedback. *IEEE Transactions on Biomedical Engineering*, 63(3):519–529, 2016.

[34] Anne-Marie Brouwer, Thorsten O Zander, Jan B F van Erp, Johannes E Korteling, and Adelbert W Bronkhorst. Using neurophysiological signals that reflect cognitive or affective state: six recommendations to avoid common pitfalls. *Frontiers in Neuroscience*, 9:136, 2015.

[35] Paul Von Bünau, Frank C. Meinecke, Franz C. Király, and Klaus Robert Müller. Finding Stationary Subspaces in Multivariate Time Series. *Physical Review Letters*, 103(21):1–4, 2009.

[36] Pradeep Shenoy, Matthias Krauledat, Benjamin Blankertz, Rajesh P. N. Rao, and Klaus-Robert Müller. Towards adaptive classification for BCI. *Journal of neural engineering*, 3(1):R13–R23, 2006.

[37] Benjamin Blankertz, Steven Lemm, Matthias Treder, Stefan Haufe, and Klaus Robert Müller. Single-trial analysis and classification of ERP components - A tutorial. *NeuroImage*, 56:814–825, 2011.

[38] David E Thompson, Seth Warschausky, and Jane E Huggins. Classifier-based latency estimation: a novel way to estimate and predict BCI accuracy. *Journal of neural engineering*, 10(1):016006, 2013.

[39] C Vidaurre and M Kawanabe. Toward an unsupervised adaptation of LDA for Brain-Computer Interfaces. *IEEE transactions on bio-medical engineering*, 58(3):587–597, 2011.

[40] Hartmut Traunmüller. Paralinguistic variation and invariance in the characteristic frequencies of vowels. *Phonetica*, 45(1):1–29, 1988.

[41] Iñaki Iturrate, Luis Montesano, and Javier Minguez. Task-dependent signal variations in EEG error-related potentials for brain-computer interfaces. *Journal of neural engineering*, 10(2):1–13, 2013.

[42] Martin Spüler and Christian Niethammer. Error-related potentials during continuous feedback: using EEG to detect errors of different type and severity. *Frontiers in Human Neuroscience*, 9(March):1–10, 2015.

[43] Iñaki Iturrate, Ricardo Chavarriaga, Luis Montesano, Javier Minguez, and José del R Millán. Latency Correction of Event-Related Potentials between Different Experimental Protocols. *Journal of neural engineering*, 11(3):036005, 2014.

[44] Perrin Magaurx, Maby Emmanuel, Daligault Sébastien, Bertrand Olivier, and Mattout Jérémie. Objective and subjective evaluation of online error correction during P300-based spelling. *Advances in Human-Computer Interaction*, 2012, 2012.

[45] Bernardo Dal Seno, Matteo Matteucci, and Luca Mainardi. Online detection of P300 and error potentials in a BCI speller. *Computational Intelligence and Neuroscience*, 2010, 2010.

[46] Hiromu Takahashi, Tomohiro Yoshikawa, and Takeshi Furuhashi. A study on combination of reliability-based automatic repeat request with error potential-based error correction for improving P300 speller performance. *Electronics and Communications in Japan*, 97(1):12–21, 2014.

[47] Matthias S. Treder, Nico M. Schmidt, and Benjamin Blankertz. Gaze-independent brain-computer interfaces based on covert attention and feature attention. *Journal of Neural Engineering*, 8(6):66003, 2011.

[48] Ben D. Sawyer, Waldemar Karwowski, Petros Xanthopoulos, and P. A. Hancock. Detection of error-related negativity in complex visual stimuli: a new neuroergonomic arrow in the practitioner's quiver. *Ergonomics*, 0139(March):1–7, 2016.

[49] Sven Hoffmann and Michael Falkenstein. Aging and error processing: Age related increase in the variability of the error-negativity is not accompanied by increase in response variability. *PLoS ONE*, 6(2), 2011.

[50] Robert Hester, Catherine Fassbender, and Hugh Garavan. Individual differences in error processing: A review and reanalysis of three event-related fMRI studies using the GO/NOGO task. *Cerebral Cortex*, 14(9):986–994, 2004.

[51] Jijun Tong, Qinguang Lin, Ran Xiao, and Lei Ding. Combining multiple features for error detection and its application in brain-computer interface. *Biomedical engineering online*, 15(1):17, 2016.

[52] Johannes Höhne, Konrad Krenzlin, Sven Dähne, and Michael Tangermann. Natural stimuli improve auditory BCIs with respect to ergonomics and performance. *Journal of Neural Engineering*, 9(4):045003, 2012.

[53] Fayeem Aziz, Hamzah Arof, Norrima Mokhtar, and Marizan Mubin. HMM based automated wheelchair navigation using EOG traces in EEG. *Journal of neural engineering*, 11(5):056018, 2014.

[54] Christoph Hintermüller, Christoph Kapeller, Günter Edlinger, and Christoph Guger. BCI Integration : Application Interfaces. In Dr. Reza Fazel-Rezai, editor, *Brain-Computer Interface Systems - Recent Progress and Future Prospects*, pages 21–41. InTech, 2013.

[55] Jana I. Münßinger, Sebastian Halder, Sonja C. Kleih, Adrian Furdea, Valerio Raco, Adi Hösle, and Andrea Kübler. Brain painting: First evaluation of a new brain-computer interface application with ALS-patients and healthy volunteers. *Frontiers in Neuroscience*, 4(NOV):1–11, 2010.

[56] Carlos Escolano, Javier Mauricio Antelis, and Javier Minguez. A telepresence mobile robot controlled with a noninvasive brain-computer interface. *IEEE transactions on systems, man, and cybernetics. Part B, Cybernetics*, 42(3):793–804, jun 2012.

[57] F Nijboer, E W Sellers, J Mellinger, M A Jordan, T Matuz, A Furdea, S Halder, U Mochty, D J Krusienski, T M Vaughan, J R Wolpaw, N Birbaumer, and A Kübler. A P300-based brain–computer interface for people with amyotrophic lateral sclerosis. *Clinical neurophysiology*, 119(8):1909–1916, 2008.

[58] Roger H. S. Carpenter and M. L. L. Willimas. Neural computation of log likelihood in control of saccadic eye movements. *Nature*, 377(6544):59–62, 1995.

[59] Julia W Y Kam, Elizabeth Dao, Patricia Blinn, Olav E Krigolson, Lara a Boyd, and Todd C Handy. Mind wandering and motor control: off-task thinking disrupts the online adjustment of behavior. *Frontiers in human neuroscience*, 6(December):329, 2012.

[60] Juliane Schäfer and Korbinian Strimmer. A shrinkage approach to large-scale covariance matrix estimation and implications for functional genomics. *Statistical applications in genetics and molecular biology*, 4(1):1–

30, 2005.

[61] Christian Andreas Kothe and Scott Makeig. BCILAB: a platform for brain-computer interface development. *Journal of neural engineering*, 10(5), 2013.

[62] Christoph Guger, Shahab Daban, Eric Sellers, Clemens Holzner, Gunther Krausz, Roberta Carabalona, Furio Gramatica, and Guenter Edlinger. How many people are able to control a P300-based brain-computer interface (BCI)? *Neuroscience Letters*, 462(1):94–98, 2009.

[63] Ivo Käthner, Andrea Kübler, and Sebastian Halder. Rapid P300 brain-computer interface communication with a head-mounted display. *Frontiers in Neuroscience*, 9:1–13, 2015.

[64] William Speier, Aniket Deshpande, and Nader Pouratian. A method for optimizing EEG electrode number and configuration for signal acquisition in P300 speller systems. *Clinical Neurophysiology*, 126(6):1171–1177, 2015.

[65] J Yordanova and V Kolev. Event-related alpha oscillations are functionally associated with P300 during information processing. *Neuroreport*, 9(14):3159–3164, 1998.

[66] J Yordanova and V Kolev. Single-sweep analysis of the theta frequency band during an auditory oddball task. *Psychophysiology*, 35(1):116–26, 1998.

[67] Canan Baar-Eroglu, Erol Baar, Tamer Demiralp, and Martin Schürmann. P300-response: possible psychophysiological correlates in delta and theta frequency channels. A review. *International Journal of Psychophysiology*, 13(2):161–179, 1992.

[68] John Polich. Updating P300: An Integrative Theory of P3a and P3b John. *Clinical neurophysiology*, 118(10):2128–2148, 2007.

[69] William J Gehring, Brian Goss, and Michael G H Coles. A neural system for error detection and compensation. *Psychological Science*, 4:385–390, 1993.

[70] Lijun Wang, Weigang Pan, Jinfeng Tan, Congcong Liu, and Antao Chen. Slowing after observed error transfers across tasks. *PLoS ONE*, 11(3):1–15, 2016.

[71] Ching Fan Sheu, Émeline Perthame, Yuh Shiow Lee, and David Causeur. Accounting for time dependence in large-scale multiple testing of event-related potential data. *Annals of Applied Statistics*, 10(1):219–245, 2016.

[72] Isabelle Guyon and Andre Elisseeff. An Introduction to Variable and Feature Selection. *The Journal of Machine Learning Research*, 3(3):1157–1182, 2003.

[73] Lorenzo Trippa, Levi Waldron, Curtis Huttenhower, and Giovanni Parmigiani. Bayesian nonparametric cross-study validation of prediction methods. *Annals of Applied Statistics*, 9(1):402–428, 2015.

[74] Markus Ojala and Gemma C. Garriga. Permutation Tests for Studying Classifier Performance. *Journal ofMachine Learning Research*, 11:1833–1863, 2010.

[75] Rodney J. Croft and Robert J. Barry. Removal of ocular artifact from the EEG: a review. *Neurophysiologie Clinique/Clinical Neurophysiology*, 30(1):5–19, 2000.

[76] Yoav Benjamini and Yosef Hochberg. Controlling the false discovery rate: a practical and powerful approach to multiple testing. *Journal of the Royal Statistical Society B*, 57(1):289–300, 1995.

[77] Thorsten O. Zander, Laurens R. Krol, Niels P. Birbaumer, and Klaus Gramann. Neuroadaptive technology enables implicit cursor control based on medial prefrontal cortex activity. *Proceedings of the National Academy of Sciences*, 113(52):14898–14903, 2016.

[78] Doreen M. Olvet and Greg Hajcak. The stability of error-related brain activity with increasing trials. *Psychophysiology*, 46(5):957–961, 2009.

[79] Robert D Flint, Zachary A Wright, Michael R Scheid, and Marc W Slutzky. Long term, stable brain machine interface performance using local field potentials and multiunit spikes. *Journal of Neural Engineering*, 10(5):056005, 2013.

[80] Beata Jarosiewicz, Anish A Sarma, Daniel Bacher, Nicolas Y Masse, John D Simeral, Brittany Sorice, Erin M Oakley, Christine Blabe, Chethan Pandarinath, Vikash Gilja, Sydney S Cash, Emad N Eskandar, Gerhard Friehs, Jaimie M Henderson, Krishna V Shenoy, John P Donoghue, and Leigh R Hochberg. Virtual typing by people with tetraplegia using a self-calibrating intracortical brain-computer interface. *Science Translational Medicine*, 7(313):313ra179—-313ra179, 2015.

[81] Jonathan Grizou, Iñaki Iturrate, Luis Montesano, Pierre-yves Oudeyer, and Manuel Lopes. Calibration-Free BCI Based Control. In *AAAI conference on Artificial Intelligence*, 2014.

[82] Enea Francesco Pavone, Gaetano Tieri, Giulia Rizza, Emmanuele Tidoni, Luigi Grisoni, and Salvatore Maria Aglioti. Embodying Others in Immersive Virtual Reality: Electro-Cortical Signatures of Monitoring the Errors in the Actions of an Avatar Seen from a First-Person Perspective. *The Journal of neuroscience : the official journal of the Society for Neuroscience*, 36(2):268–79, 2016.

[83] Martin E. Maier, Marco Steinhauser, and Ronald Hübner. Effects of response-set size on error-related brain activity. *Experimental Brain Research*, 202(3):571–581, 2010.